Stabilization of bio-oil from simulated pyrolysis oil using sulfided NiMo/Al<inf>2</inf>O<inf>3</inf> catalyst

Fuel 353 (2023) 129094

Contents lists available at ScienceDirect

Fuel

journal homepage: www.elsevier.com/locate/fuel

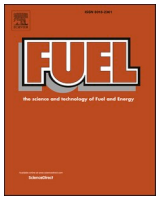

Full Length Article

Stabilization of bio-oil from simulated pyrolysis oil using sulfided NiMo/Al_2O_3 catalyst

Elham Nejadmoghadam [a], Abdenour Achour [a], Pouya Sirous-Rezaei [a], Muhammad Abdus Salam [a], Prakhar Arora [b], Olov Öhrman [b], Derek Creaser [a], Louise Olsson [a,*]

[a] Chemical Engineering Division, Competence Centre for Catalysis, Chalmers University of Technology, Gothenburg 41296, Sweden
[b] Preem AB, Gothenburg SE-417 26, Sweden

ARTICLE INFO

Keywords:
Simulated pyrolysis oil
Stabilization
Catalytic hydrotreatment
Solid product nature
Sulfided NiMo/Al_2O_3 catalyst

ABSTRACT

Pyrolysis oil comprises compounds with a broad range of functional groups making its thermal/catalytic upgrading challenging due to the formation of undesired char. In this context, the current contribution addresses the thermal and catalytic hydrotreatment of a simulated pyrolysis oil containing all the representative groups of compounds under bio-oil stabilization conditions (180–300 °C, 60 bar, 4 h) using sulfided NiMo/Al_2O_3. The effect of reaction conditions and different oxygenated organic compounds on the yields and properties of products was compared thoroughly. Interestingly, a correlation between the presence/absence of oxygenated furan and sugar compounds was found to significantly affect the yield of liquid product containing stabilized compounds. The presence of such compound groups significantly enhances the solid formation via oligomerization and polymerization reactions. To gain further insight, the solid products were analyzed/characterized in detail to elucidate their characteristics by extracting them into a dimethyl sulfoxide (DMSO) soluble and insoluble solid fraction. It was found that in the presence of NiMo/Al_2O_3, increasing temperature from 180 to 300 °C enhances the formation of liquid product due to transformation of some of the soluble solids, while for experiments without the catalyst, the formation of solids was significantly higher. Oppositely, during heating up to 180 °C, no solids were found in the case without the catalyst, however the presence of the catalyst during heating resulted in solid formation due to various catalytic reactions that promoted char formation. Analysis of solids revealed that the structure of soluble solids at lower temperatures (180 °C) using the catalyst was closely related to sugar derivatives, whereas the corresponding insoluble solids with higher molecular weight were not fully char-like developed. However, at higher temperatures, the soluble and insoluble solid compositions were found to contain aliphatic compounds and fully developed char, respectively. Therefore, the stabilization of furan particularly with attached carbonyl groups and sugars derivatives in pyrolysis oil is of great importance to improve upgrading efficiency.

1. Introduction

The usage of renewable resources and developing efficient processes for converting them into renewable fuels and bio-based chemicals has become of great interest in recent years [1]. Biomass is one of the main renewable resources which is processed through various thermochemical techniques, e.g., fast pyrolysis, leading to a bio-oil, so-called pyrolysis oil [2]. Pyrolysis oil obtained from biomass does not resemble a typical crude oil and is an extremely complex mixture that contains hundreds of organic compounds including oxygen-containing organic groups (e.g., aldehydes, ketones, furans, sugars, carboxylic acids, and phenols) and up to 30 wt% water which leads to its high thermal instability and propensity for polymerization and consequently formation of solids/char. Therefore, it needs to be upgraded and hydrodeoxygenation (HDO) is the most promising method for this purpose. However, the conversion of pyrolysis oil to biofuels via reduction of its excessive oxygen content requires it to be heated [3]. HDO is typically performed at elevated temperatures with high hydrogen pressure and in the presence of a suitable catalyst [4].

During hydrotreatment process, solid/char formation is a major side-reaction causing a lower yield of desired liquid products and deactivation of the catalyst [5–7]. To tackle this issue, a two-stage process can be

* Corresponding author.
E-mail address: louise.olsson@chalmers.se (L. Olsson).

https://doi.org/10.1016/j.fuel.2023.129094
Received 1 March 2023; Received in revised form 8 June 2023; Accepted 23 June 2023
Available online 13 July 2023

used that applies an additional stabilization step under milder conditions (150–300 °C) intended to suppress the solid/char formation by stabilizing the pyrolysis oil via conversion of reactive compounds into more stable compounds. This mild treatment is then followed by further hydrotreatment at more severe conditions (300–500 °C) aiming at full deoxygenation [6,8–15].

Stabilization of pyrolysis oil involves a complex network of numerous different reactions originating from the complicated composition of bio-oil, including hydrogenation, deoxygenation, esterification, dehydration, etc. [6,16–20]. On the other hand, unfavorable cross-linking and polymerization reactions [21,22] cause the formation of heavy oligomeric compounds and ultimately char which makes it difficult to gain insight into the reaction pathway of individual compounds, and in particular their role on solid formation. Accordingly, the mild hydrotreatment of mixed model compounds, intended to simulate pyrolysis oil, has been studied in recent years to provide information about how composition affects selectivity, which helps to reveal the reaction mechanisms involved in real pyrolysis oil mild hydrotreatment [3,23–27]. Boscagli et al. [24] studied the mild hydrotreatment of the light fraction of straw derived-pyrolysis oil containing oxygenated compounds with low molecular weight, such as sugar derivatives, phenol derivatives, furans, ketones, aldehydes, acids, and alcohols. All experiments were conducted at 250 °C and 8 MPa hydrogen pressure using various catalysts, $NiCu/Al_2O_3$, Ni/ZrO_2, Ni/SiO_2, Ni/TiO_2, Ni/Al_2O_3. Significant decrease in the oxygen content of stabilized oil (20 wt %) with better performance of $NiCu/Al_2O_3$ due to hydrodeoxygenation reactions were reported. It was also observed for all nickel-based catalysts, a good selectivity for the hydrogenation of olefinic groups, but not for the ketones. Han et al. [3] studied the mild hydrotreatment of a mixture of hydroxyacetone, furfural, and phenol as a simulated pyrolysis oil and the interactions among them using a Ni/SiO_2 catalyst at 160–240 °C and 3.5 MPa H_2. According to their observations, the conversion of hydroxyacetone and especially phenol was inhibited by furfural due to its strong adsorption on the surface of the catalyst [3]. In another work performed by Wan et al. [23], a mixture of acetic acid and p-cresol was used to mimic pyrolysis oil using Ru/C at 300 °C and 48 bar H_2 in which hydrogenation of acetic acid was suppressed by the presence of p-cresol. Although, HDO of p-cresol was promoted via dehydration and high selectivity for methylcyclohexane [23]. Chen et al. [25] elaborated on the hydrogenation behaviors of some typical compounds including guaiacol, phenol, acetic acid, furfural, and hydroxyacetone over bimetallic catalysts (Pt-Ni, Pt-Fe, Pd-Ni and Pd-Fe,) supported on SiO_2 at 240–300 °C with ethanol which acts as a hydrogen donor. The distribution of liquid products indicated that hydrogenation of the aldehyde group in furfural occurred initially. It was followed by the furan ring hydrogenation, while phenol and guaiacol, the representative phenolic compounds, underwent hydrogenation of their methoxy group first and then the phenol ring to produce alcohol (cyclohexanol). This alcohol was an intermediate to produce ketone (cyclohexanone) via keto-enol tautomerism as well. In addition, hydrogenation of hydroxyacetone and condensation of acetic acid and produced alcohols resulted in the formation of their corresponding alcohol and ester, respectively [25]. Ni/CMK-3 catalyst was used by Xu et al. [26] for in-situ hydrogenation of mixed model compounds (acetone, acetic acid, furfural, o-cresol, ethanediol and water) of pyrolysis oil using various hydrogen donor solvents, including methanol, ethanol, and formic acid at 230 °C. It was found that solvents affect the conversion of model compounds and the course of reaction, where esterification reactions occurred between acetic acid and the alcohol hydrogen donors. However, in the case of formic acid, the phenol conversion increased from 21 to 66% whereas the conversion of acetic acid was significantly reduced (64 to 12%). Also, another observation was that the increase in conversion of model compounds coincided with increasing methanol concentration and thus the solvent mixture of water and methanol was selected for better conversion due to hydrogenation as well as esterification reactions. In another study [27], the mixture of eugenol, guaiacol, phenol, furfural, acetic acid, and water (a simulated pyrolysis oil) and a mixture of phenolic compounds were evaluated during mild catalytic hydrotreatment using a Ru/SBA-15 catalyst in combination with the isopropanol solvent. The results showed effective conversion of phenolic compounds into alcohols (cyclohexanol and its derivatives) at 120 °C. Furthermore, catalyst deactivation was observed during only stabilization of real pyrolysis oil but not simulated pyrolysis oil. Evaluation of the above-mentioned studies indicates that not all the main oxygenated compounds simultaneously present in a pyrolysis oil has been considered in these simulated pyrolysis feedstock mixtures and the composition of stabilized oils was mainly highlighted.

However, the knowledge about how pyrolysis oil converts to solids at low temperatures is also indispensable. The molecular structure of the oxygenated compounds plays a decisive role in their tendency to polymerize. To elucidate the reaction mechanism for polymerization, some studies have been investigated using model compounds [21,28–31]. The effect of sugar on solid/coke formation under mild conditions by adding levoglucosan into a pyrolysis oil has been reported to result in severe coke formation due to cross-linking with other compounds in the absence of a catalyst. However, the presence of a sulfided $NiMo/Al_2O_3$ catalyst could prevent the formation of additional coke [28]. The presence of carboxylic acids in a pyrolysis oil mixture has been shown to behave as acid catalysts for promoting polymerization during thermal hydrotreatment. However acetic acid, due to its weak acidity was found to have an insignificant influence on enhancing polymerization [29–31]. The cross-polymerization between furfural and phenolics during thermal treatment at 200 °C, and 30 bar N_2, was boosted by the presence of stronger acids (H_2SO_4 and benzoic acid), as reported by Xu et al. [29]. Observations by Sun et. al [21] illustrate that cross-polymerization between furans and phenolics occurred even during a transient heating process taking 0.5 h up to 200 °C with higher reactivity of furans towards polymerization. Cross-polymerization between furans and carbohydrates occurring during thermal treatment at 200 °C and 40 bar N_2 was also investigated and confirmed. The polymer from the sugars was more aliphatic than that from furans and the presence of acetic acid promoted the formation of the insoluble polymer [30]. In another study [32], Hydroxy methyl furfural (HMF) and furfural were found to be the most effective polymerization agents compared to vanillin, guaiacol, xylose, methanol, hydroxyl acetone, furan, and furfuryl alcohol for significantly enhancing the solid yield when added individually to pyrolysis oil. But, there is still a lack of understanding regarding the solid product characterization and the contribution of different oxygenated groups individually to form heavy compounds and thereby solids/char during both thermal and catalytic hydrotreatment.

In most studies of processes for stabilization of pyrolysis oil and its model compounds noble metal catalysts are employed due to their high hydrogenation efficiency to eliminate the highly reactive compounds under mild conditions [6,8,15,25,33–37]. Despite their good performance, their high cost may restrict their application in some cases. Furthermore, they are easily poisoned by sulfur in conventional crude oils. As a result, their use can be impractical in processes that co-process conventional crude and bio-oils [38]. Sulfided NiMo catalysts are well-established, cost-effective, and sulfur-resistant catalysts, typically used at high temperatures (greater than350 °C), but still could be sufficiently active at lower temperatures [8]. Kadarwati et al. [28] employed typical HDO catalyst (sulfided $NiMo/Al_2O_3$ catalyst) for stabilization of pyrolysis oil at low temperatures (150–300 °C). It was found that the catalyst plays an important role in reducing the solid formation and oxygen content by ca. 55.5% at 300 °C compared to the catalyst-free experiment. However, their study did not reveal detailed information about the effect of the pyrolysis oil composition on solid/char formation as well as their characteristics in the presence of such catalyst [28].

As a step toward gaining further insight into solid/char formation in stabilization process, in this study, a detailed investigation of pyrolysis oil during mild hydrotreatment using a sulfided $NiMo/Al_2O_3$ catalyst

has been explored. Accordingly, to simulate pyrolysis oil more realistically, a comprehensive mixture containing a representative from each main oxygenated group comprising the different functional groups has been opted and to the best of our knowledge for the first time a set of experiments by removing the reactants from the mixture one by one, were carried out to be able to probe their roles in the product distribution in different phases and particularly their conversion to char/solid. A mixture of guaiacol, levoglucosan, acetic acid, Hydroxymethylfurfural (HMF), benzaldehyde, and hydroxyacetone was adopted as a simulated pyrolysis oil representing phenols, sugars, carboxylic acids, furans, aldehydes, and ketones, respectively. In addition, for the first time according to our knowledge we are examining the effect of the heating period on product selectivity in the presence and absence of catalyst. It is very important to understand how the heating process should be designed in order not to form char that could plug the tubing or catalyst bed and increase the pressure drop. Furthermore, the yields and properties of the solid product were determined by extracting them further into soluble and insoluble (char-like material) fractions to study their chemical structure distribution as a key factor for developing the stabilization process. To determine the mechanisms of the thermal conversion of simulated pyrolysis oil components, experiments in the absence of the catalyst (blank) under identical reaction conditions were also conducted. Liquid and solid/char products obtained from both catalytic and blank experiments were analyzed by GC–MS, Karl Fischer, MALDI-TOF, HSQC-2D-NMR, and CHOS elemental analysis. The product properties were used to determine the hydrogenation activity of the sulfided $NiMo/Al_2O_3$ catalyst in comparison with blank experiments·NH_3-TPD, BET, SEM, TEM and ICP analysis were also applied for the characterization of the catalyst used in this study.

2. Experimental

2.1. Catalyst synthesis

A Nickel-Molybdenum (NiMo) catalyst supported on ϒ-alumina was applied for the mild hydrotreatment study. It was prepared through a conventional incipient wetness co-impregnation of ϒ-alumina (Puralox SCCA 150/200, Sasol) with an aqueous solution containing the required amounts of $Ni(NO_3)_2{\cdot}6H_2O$ and $(NH_4)_6Mo_7O_{24}{\cdot}4H_2O$ (Sigma-Aldrich). First the ϒ-alumina support was calcined at 550 °C for 8 h, followed by its impregnation with 3.6 and 13.2 wt% loadings of Ni and Mo, respectively (determined by ICP analysis). Thereafter the catalyst was dried first at 60 °C overnight for 12 h and then at 110 °C for 12 h, with subsequent calcination at 550 °C for 12 h using a heating rate of 2 °C min^{-1}. The prepared NiMo/ϒ-alumina catalyst was sulfided with dimethyl disulfide (DMDS) at 340 °C and 20 bar hydrogen for 4 h in a Parr autoclave reactor to activate it before starting the reaction. The resulting sulfide ϒ-alumina-supported Ni and Mo catalyst will here on be abbreviated as $NiMo/Al_2O_3$. Details regarding catalyst characterization techniques and all materials used in this study are given in the supplementary Sections 2.1 and 2.2.

2.2. Hydrotreatment experimental protocol

The catalytic and thermal mild hydrotreatment experiments were conducted in a 450 ml Parr autoclave reactor system. In each experiment, 150 ml of hexadecane (≥99%, Sigma-Aldrich) and a solution containing the mixture of each 1 g of acetic acid, hydroxyacetone, benzaldehyde, guaiacol, HMF, and levoglucosan was introduced into the reactor along with 1 g of presulfided catalyst (or without catalyst). The same amount of each oxygenated compound was used in the mixture (simulated pyrolysis oil) to enable a comparison of the effect of each oxygenated group at the same concentration, even though in a real pyrolysis oil the ratio of these groups can differ greatly. The H/C and O/C molar ratio for the simulated pyrolysis oil is 1.3 and 0.5, similar to real fast pyrolysis bio-oils (1.3 and 0.4, respectively). 166 uL DMDS was also added to sustain the catalyst in its sulfide state during the reaction. After evacuating the reactor by pressurizing/depressurizing it (three times first with nitrogen and then with hydrogen gas), the reactor was charged with 30 bar of hydrogen gas and heated to the reaction temperature (180–300 °C) at an average heating rate of 12 °C/min while stirring at 1000 rpm. The effect of the replacement of N_2 atmosphere by using H_2 on catalytic upgrading of a pyrolysis oil has been studied earlier [39]. The total replacement of N_2 atmosphere with H_2 decreased the product molar O/C ratio, due to the H_2-atmosphere promoting hydrodeoxygenation and hydrocracking of oxygenated compounds present in the pyrolysis oil. Accordingly, in our study, the mild catalytic hydrotreatment of simulated pyrolysis oil was conducted in the presence of H_2 gas to effectively decrease the O/C ratio of the stabilized oil. To analyze the effect of the heating process, after reaching the setpoint, 180 °C, the reaction was stopped by rapid cooling to room temperature which took about 11 min. However, for other experiments, it was maintained at the final temperature for a duration of 4 h. During heating up to reach the specific setpoint, the pressure gradually increased from 30 bar to 45.2, 45.5, 47.8, and 51.4 bar at the final reaction temperatures of 180, 210, 250, and 300 °C, respectively. To maintain the same pressure in all experiments for the final 4 h reaction stage at set temperature, additional hydrogen was fed to reach 60 bar while continuously stirring, after the final setpoint temperature was reached. For comparison, blank experiments without the catalyst (all other conditions identical) were conducted. After the pre-set reaction time (4 h), the reactor was rapidly cooled down to room temperature and then depressurized. The vessel containing the hydrotreated simulated pyrolysis oil was weighed and compared with the weight of the feed solution and empty vessel. The residual difference from this comparison was about 1.3–1.8 wt%, indicating that any losses and/or gas formation were small. The detailed information regarding liquid and solid product extraction methods can be found in the supplementary Section 2.3.

The GC/MS detectable liquid product yields were measured by an internal standard calibration method. Experiments were carried out in triplicates, to ensure the reproducibility of the data. Accordingly, the measured weights of the light liquid product, total solid product, insoluble solid, and water were used for product yield calculations (%w/w), according to Eq. (1–4).

$$\text{Yield GC/MS detectable liquid product}(\%) = \frac{\text{Mass of light products detcted by GC/MS}}{\text{Mass of simulated pyrolysis oil feed}} \times 100\% \quad (1)$$

$$\text{Yield Solid product } (\%) = \frac{\text{Mass of solid product}}{\text{Mass of simulated pyrolysis oil feed}} \times 100\ \% \quad (2)$$

$$\text{Yield Insoluble solid } (\%) = \frac{\text{Mass of insoluble solid}}{\text{Mass of simulated pyrolysis oil feed}} \times 100\ \% \quad (3)$$

$$\text{Yield Water } (\%) = \frac{\text{Mass of water}}{\text{Mass of simulated pyrolysis oil feed}} \times 100\ \% \quad (4)$$

$$\text{Yield unreacted simulated pyrolysis oil}(\%) = \frac{\text{Mass of remain reactants detected by GC/MS}}{\text{Mass of simulated pyrolysis oil feed}} \times 100\ \% \quad (5)$$

In addition, GC/MS undetectable compounds, consisting of high molecular weight oligomers soluble in the reaction solution, were produced which from here on will be referred to as the 'liquid oligomeric products'. Their yield was calculated from difference of the yield of other products, according to Eq. (6):

$$\text{Yield liquid oligomeric products}(\%) = 100 - \text{Yield GC/MS detectable liquid product} - \text{Yield solid product} - \text{Yield water} \quad (6)$$

Various analytical methods including gas chromatography-mass spectroscopy (GC–MS), volumetric Karl Fisher titration, two dimensional heteronuclear single-quantum coherence (HSQC)-NMR, Matrix Assisted Laser Desorption Ionization Time of Flight Mass Spectroscopy (MALDI-TOF MS) and CHOS elemental analysis were applied for analysis of the different product phases obtained from the mild hydrotreatment process. Their details are discussed in the Supplementary Section 2.4.

The activity/reusability of freshly and regenerated sulfided NiMo/Al_2O_3 catalyst was compared via two consecutive experiments at identical reaction conditions (180 °C, 60 bar H_2 for duration of 4 h using 1 g catalyst). The catalyst regeneration involved oxidizing the insoluble solid/char along with the catalyst obtained from first experiment in air at 500 °C for 5 h to combust the solid. Due to small loss of catalyst material during filtration, 0.9 g of spent catalyst was recovered from the original 1 g of catalyst charged. Therefore, to provide 1 g of spent catalyst for a second consecutive experiment, another run at identical conditions with fresh catalyst after sulfidation was conducted and the same procedure for regeneration was followed. The two identical runs using fresh catalyst demonstrated a high level of reproducibility with solid yields of 13.6 and 14.1 wt%, respectively. The catalyst reusability was evaluated by a subsequent experiment with the regenerated catalyst (1 g) using the same conditions described for the fresh catalyst earlier.

3. Results and discussions

3.1. Catalyst characterization

In this study the effect of adding a NiMo/Al_2O_3 catalyst during mild hydrotreatment was studied. The NiMo/Al_2O_3 catalyst was characterized and the specific surface area, pore volume, and mesopore sizes are illustrated in Table S1. XRD was performed and all peaks corresponding to Al_2O_3 were also observed in the NiMo/Al_2O_3 catalyst (Fig. S2). No peak for NiO was found, indicating a good dispersion of the Ni or due to the low loading of Ni. However, a noticeable peak for MoO_3 at $2\theta = 26.7^\circ$ was visible because of the higher loading of Mo on the support (Fig. S2) [40]. The acidity of the catalyst sample was measured using NH_3 TPD and the results are shown in Fig. S3 and Table S1. The morphology of the sulfided NiMo/Al_2O_3 catalyst was examined from SEM and TEM images, as depicted in Fig. S4. The SEM image of NiMo/Al_2O_3 demonstrates microspheres with particle sizes ranging from 0.1 to 2.0 μm. The TEM image shows the dispersion of typical layers of Ni promoted MoS_2 crystallites [41] with an interlayer distance of 0.62 nm corresponding to the (0 0 2) basal planes of MoS_2.

3.2. Effects of reaction temperature

3.2.1. Conversions and product distribution yields

At first, mild hydrotreatment of simulated pyrolysis oil was performed to obtain stable intermediates/products. The effect of temperature on the hydrotreatment was examined with the NiMo/Al_2O_3 catalyst at 180, 210, 250, and 300 °C and keeping all other conditions constant (60 bar H_2 in a batch reactor for 4 h). For comparison, blank experiments were conducted without the catalyst, but under the same conditions to study the thermal, non-catalytic reactions in detail. The evolution of simulated pyrolysis oil conversion and product distribution as a function of temperature in catalytic and thermal hydrotreatment (blank) experiments are illustrated in Fig. 2 and Table S2, respectively.

The NiMo/Al_2O_3 catalyst mainly affected the conversion and distribution of products in different fractions compared to the blank experiments. In the presence of the catalyst, HMF, levoglucosan, and hydroxyacetone were nearly converted to 100% at 180 °C. The conversion of other reactants (acetic acid, benzaldehyde, and guaiacol) showed an increasing trend with elevated reaction temperature. Benzaldehyde conversion remarkably improved from 17.5% at 180 °C to 93.5% at 210 °C and became fully converted at 250 °C. These observations are in agreement with previous studies reporting 100% conversion of aldehydes and small ketones in pyrolysis oil hydrotreatment at 250 °C using a Pd/C catalyst [42] and at the temperature range lower than 180 °C for ketone using Ni–Cu/SiO_2–ZrO_2 catalyst [5]. From 180 °C, acetic acid conversion increased slowly and reached the maximum conversion at 300 °C (97%). The phenolic compound (guaiacol) in the simulated pyrolysis oil mixture showed the lowest conversion at mild conditions, 17% at 180 °C to 31% at 300 °C, which is in line with previous literature [28].

In addition, in the presence of the catalyst with the temperature increment, the yield of the liquid product increased coinciding with a decreasing fraction of unreacted simulated pyrolysis oil. The formation of liquid products is favored up to 250 °C accompanied by a reduction in solid yield (Fig. 2). The water content first slightly decreased in the temperature range of 180–210 °C, which might be ascribed to a higher rate of hydrolysis reactions at up to 210 °C [20].

The liquid product is composed of GC detectable and undetectable compounds corresponding to light and heavy oligomeric compounds produced during hydrotreatment (red-box inserted inside each figure). Since GC/MS is limited to detecting only low molecular weight compounds with high volatility, heavy compounds formed due to condensation and subsequent oligomerization reactions were not detected by GC/MS.

In presence of the catalyst, increasing the temperature from 180 °C to 300 °C ameliorated the yield of GC detectable liquid products resulting in a more than 2-fold increase, whereas it reduced the liquid oligomeric product yield. The lowest fraction of oligomeric liquid products (1.2 wt %) was obtained at the highest temperatures i.e., 300 °C. This is due to the catalyst promoting not only more dehydration and hydrogenation reactions [43], giving a high amount of water and hydrocarbons, but also hydrocracking reactions rather than polymerization and condensation reactions at higher temperatures (will be evaluated further in Section 3.2.2).

The experimental data, in agreement with literature, shows that the solid product was formed under all reaction temperatures during mild hydrotreatment [6] and reduced at higher temperatures with and without the catalyst (Fig. 1 and Table S1). However, the solid formation was more intense in the absence of the catalyst and particularly at lower temperatures. The solid product will be further discussed and characterized in Section 3.2.2.

Moreover, it could be concluded that the conversion of simulated pyrolysis oil to liquid product is nearly inversely related to the solid yield. Increasing the liquid product yield at elevated temperature, is accompanied by the reduction in solid product content as decomposition, hydrogenation, and HDO reactions become increasingly dominant. Hence, the solid precursors are converted to more stable compounds instead. However, a slightly higher solid yield was obtained at 300 °C compared to 250 °C in presence of the catalyst (Fig. 2) which might be due to further polymerization of more stable phenolic compounds at this temperature contributing to solid formation. Studies by Kadarwati et. al on mild hydrotreatment of pyrolysis oil using sulfided CoMo/Al_2O_3 catalyst reported a similar decreasing trend for solid yield by elevating the temperature [28]. However, an increasing trend for solid yield was obtained using a sulfided NiMo/Al_2O_3 catalyst under the same reaction conditions [28]. This contrasting report is probably due to the different reaction conditions (3 h and 100 bar H_2), ratios of masses of feed intake to catalyst (10 compared to 6 in our study), and the lower H_2 pressure in this study. It could also be related to the different ratio of certain selected oxygenates present in simulated pyrolysis oil compared to the real pyrolysis oil used in the literature study. For this enhancement in

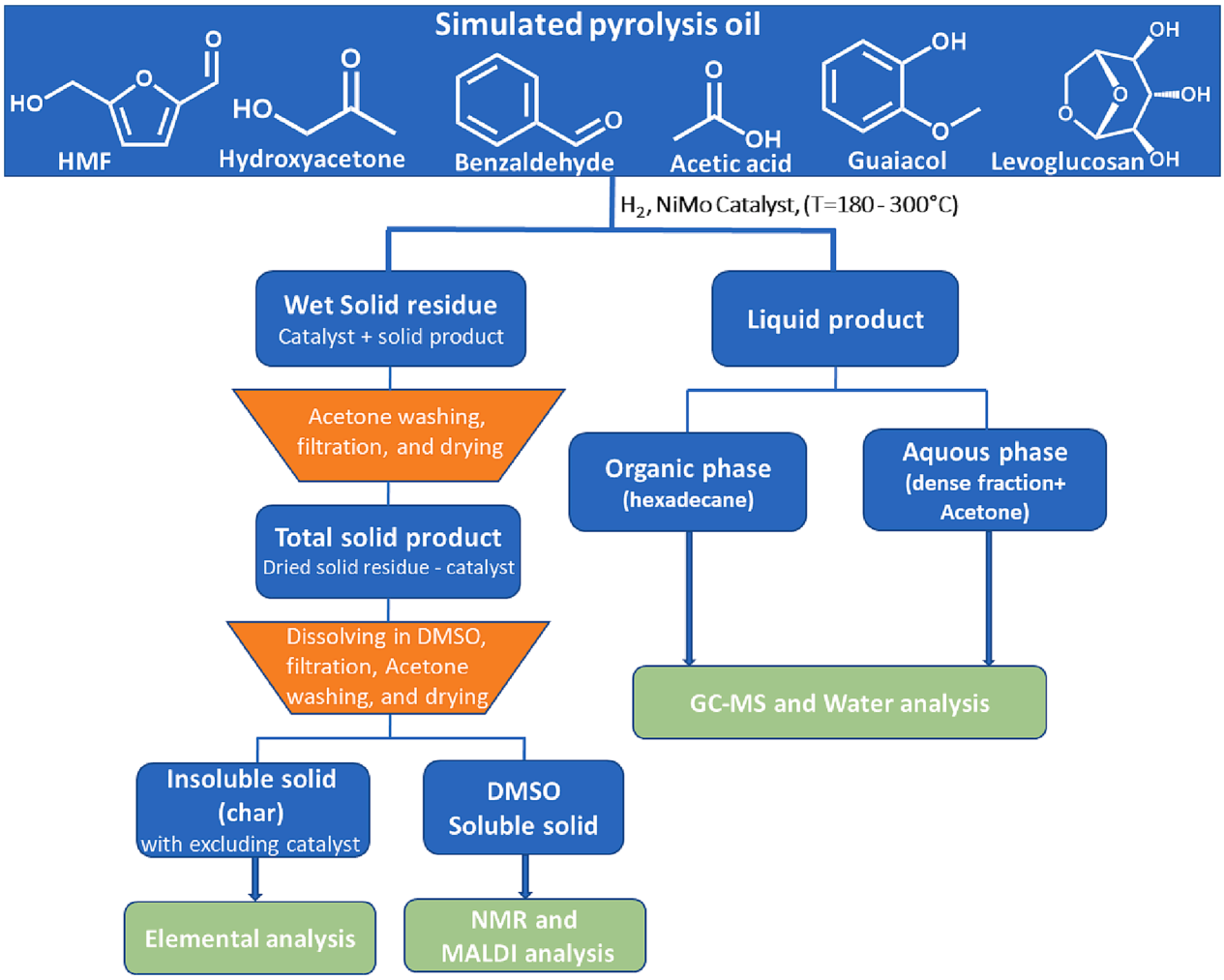

Fig. 1. Scheme of the steps for collecting products and their characterization.

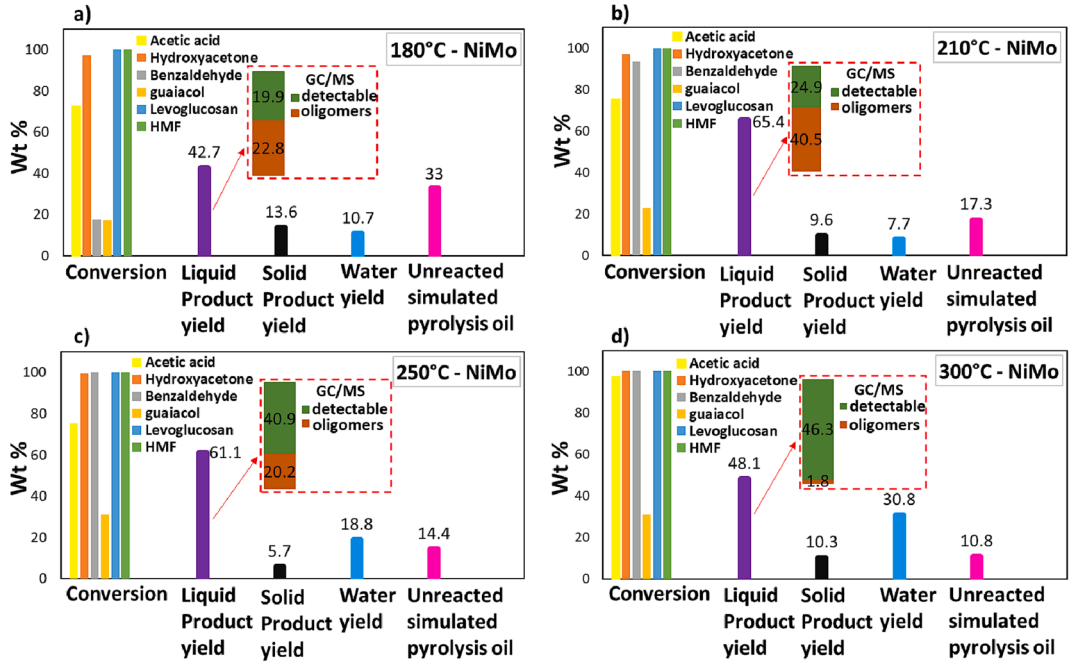

Fig. 2. Effect of reaction temperature on conversion of different oxygenated compounds in simulated pyrolysis oil and product yield (wt%). Reactions were performed under 60 bar H_2 for 4 h and 1 g $NiMo/Al_2O_3$ catalyst. a) 180 °C b) 210 °C c) 250 °C d) 300 °C.

the solid content with temperature, the secondary polymerization of the intermediate fragments produced from the cracking reactions clearly dominates [44,45]. The conversion of simulated pyrolysis oil and product distribution during thermal hydrotreatment are given in the Supplementary Section 3.1.

3.2.2. Liquid product compositions

The light organic compounds produced during mild catalytic and thermal hydrotreatment of simulated pyrolysis oil were qualitatively quantified using GC–MS analysis. For simplicity, oxygen-free compounds (hydrocarbons), and oxygenated compounds in the liquid products were classified into 8 groups, namely oxygen-free, ketone, acid, phenol, alcohol, furan (furan-ring compounds), ester, and other oxygenates that contained multiple oxygen groups. Hydrocarbons (or oxygen-free) mainly included benzene derivatives (e.g., toluene), however, compounds containing multiple oxygen groups primarily featured sugars, phenolics, and aldehyde derivatives or their combinations. Details regarding the different detected components can be found in Tables S3–S6. During mild hydrotreatment, the simulated pyrolysis oil, and reactive intermediates underwent condensation reactions giving multiple oxygen group compounds detected by GC (Tables S3–S6) and likewise, secondary reactions formed heavy oligomers in the liquid phase, which also was observed by Xu et al. [31]. Fig. 3 compares the liquid product distribution in the presence and absence of the catalyst based on the quantification of the GC–MS identified light products as a function of temperature. The catalyst had a strong influence on the course of hydrocracking, hydrogenation, esterification, and HDO reactions of reactive compounds, and indeed stabilization of the simulated pyrolysis oil compared to the same blank experiments. This was reflected by the formation and increase of alcohol, hydrocarbon, and ester products when increasing the temperature. In addition, the increased temperature also resulted in the reduction in the yield of multiple oxygen group compounds as precursors for formation heavy compounds in the catalytic hydrotreatment (Fig. 3 and S5, and Tables S3–S6). Moreover, the yield of liquid oligomer compounds underwent a sharp decrease due to their formation being prevented or hydrocracking converting them to lighter compounds, particularly at 300 °C (Fig. 2).

In the blank experiments, almost no HDO reactions occurred, resulting in a very low yield of oxygen-free products compared to the catalytic reactions at the same reaction temperature (see Fig. 3). Moreover, compared to the catalytic experiments less selectivity towards light liquid products at all reaction temperatures was seen. It can be inferred that in the absence of the catalyst, the reaction pathways forming heavy compounds via cross-polymerization of reactive free radicals is favored [21], in line with the higher yield of the liquid oligomer fraction (defined as liquid not detectable by GC–MS). Herein, the rate of hydrogenation is low compared to the rate of polymerization reactions leading to a rise in the formation of higher molecular weight compounds and eventually char. Kadarwati et. al also reported the occurrence of undesirable side reactions e.g., cross-linking and

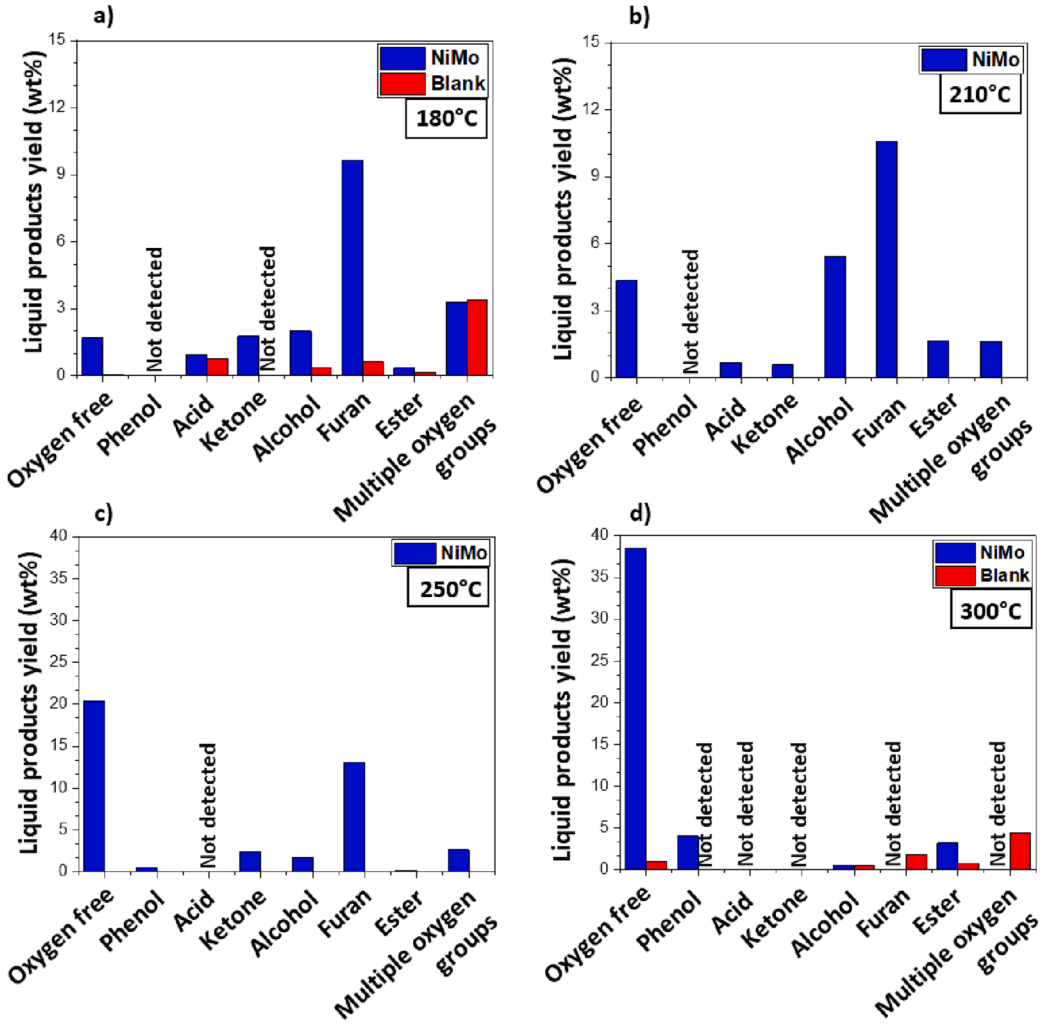

Fig. 3. Light (GC detected) product distribution (wt%) via thermal and catalytic hydrotreatment of simulated pyrolysis oil using NiMo/Al_2O_3 catalyst, a) 180 °C b) 210 °C c) 250 °C d) 300 °C, without catalyst a) 180 °C d) 300 °C.

polymerization during pyrolysis oil stabilization using Ru/C at 250 °C [46]. Moreover, no reactive aldehyde intermediates were detected in the light fraction of the liquid product, indicating either this group is easily stabilized by hydrogenation in the presence of the catalyst [42] or they strongly contribute to condensation reactions [5]. The results in Fig. 3 also indicates that esterification reactions occurred at lower temperature and particularly 210 °C, due to a reaction between acid and alcohol. In addition to acetic acid, acid intermediates (mostly consisting of benzoic acid in Tables S3 and S4) were produced as well, which then can also react with alcohols to form corresponding esters. The reason for acid formation at a lower temperature will be further discussed in the next paragraph based on the GC–MS data of liquid products. At the low temperatures (180 and 210 °C), the light phenolic compounds were not detected by GC–MS (Tables S2 and S3) which indicates the presence or absence of the catalyst practically does not affect the light phenolic compound formation. However, at the highest temperature of 300 °C, in the presence of the catalyst, guaiacol conversion via demethoxylation, direct HDO, and dehydration produced phenol, catechol and aromatic hydrocarbons (Fig. S2 and Table S6). Meanwhile, at 300 °C, the NiMo/Al_2O_3 catalyst actively catalyzes deoxygenation with the highest oxygen-free yield, and full conversion of reactive intermediates (ketones and aldehydes) mainly into light fractions, thus, avoiding extensive solid formation. A strong correlation exists between temperature and the oxygen content of the light liquid product. At 250 °C instead, a hypothesis is that hydrolysis reactions are favored that would likely take place concurrently with esterification, therefore the rate of hydrolysis is higher than the oligomerization reactions as evident from the GC–MS results with a higher yield of esters in the light liquid phase and lower solid and water yields. These results are in line with the work by Gunawan et al. who observed simultaneous hydrolysis and esterification of fast pyrolysis oil during mild hydrotreatment at 70–170 °C using the acidic Amberlyst-70 catalyst [20]. Furthermore, hydrocarbon yield approximately doubled as the temperature was raised from 250 to 300 °C, whereas alcohol yield declined. These GC–MS results could be presumably related to the increase of water content by alcohol dehydration and HDO reactions. Another important observation and obvious difference among the reactions with and without the catalyst is the yield of furan group products. The NiMo/Al_2O_3 catalyst could effectively catalyze the transformation of HMF at lower temperatures (180, 210, and 250 °C), into products with furan rings but with mostly hydrogenation of the attached oxygen-functional groups particularly at 250 °C (Tables S3–S5) and eventually converting them to hydrocarbons at the highest temperature of 300 °C (Fig. 3 and S2, and Table S6). It should be noted that at 180 and 210 °C, very reactive furan ring compounds with carbonyl functional groups are predominant. However, by increasing temperature up to 250 °C, the furan group products were more stable and mostly consisted of a furan ring free of functional groups, indicating that in the presence of the catalyst the furan ring is most recalcitrant to deoxygenation compared to its attached carbonyl groups (Tables S3–S5). These results are in agreement with Nolte et al. [47] who observed that furan ring deoxygenation in HMF is more resistant compared with its carbonyl and hydroxyl groups. It should be noted that, the higher content of unsaturated groups in the liquid product could be due to limited H_2 activation by NiMoS particularly at 180 °C. Also, accordingly fewer sulfur vacancies are generated to carry out HDO [48]. This explanation is in line with more unsaturated compounds being observed at low temperature (180 °C) compared to less of the various unsaturated compounds at higher temperatures (300 °C).

Interestingly though, in the absence of the catalyst, the yield of the furan group products was not comparable to that in the presence of the catalyst at the same reaction temperatures. The lack of furan group products is likely due to polymerization reactions during thermal hydrotreatment leading to the opening of the furan ring [21,32] and/or formation of humin [49–51]. It results in the production of reactive intermediates as a key initiator for the cross-polymerizations, which facilitate the polymerization reactions and thus could be a potential/possible reason for increasing the solid yield and the oligomers not detected by GC–MS (Fig. 1). However, since the consumption of furans only occurred in the absence of the catalyst, their opening and subsequent reaction apparently occurs by reaction with other reactive oxygenate intermediates that are more prevalent without the catalyst. A correlation between the distributions of light compounds in the liquid product via GC–MS data and the physical appearance of the liquid product was also found. Among all tested temperatures, the liquid product with catalyst at 300 °C was clearest and comparable to petroleum fuels as illustrated in Fig. S6a. This result could pertain to the absence of furan group compounds, and the highest yield of oxygen-free compounds, as well as the lack of large oligomeric compounds containing furan and sugar groups at the highest temperature, since the color of hydrotreated/upgraded pyrolysis oil with a high degree of hydrodeoxygenation and hydrocracking is almost transparent [52]. While at lower temperatures (180 and 210 °C), the liquid phase was rich in furans, particularly the catalytic experiment products. In addition, different sugar compounds (classified as multiple oxygen group products) were also seen which could be attributed to the yellow color of the liquid product sample [49].

A van Krevelen plot serves as a beneficial visual tool for understanding how the elemental composition of the liquid products is influenced by catalyst and process conditions. The physicochemical properties of the liquid products obtained from thermal and catalytic hydrotreatment at 180 °C and 300 °C, such as elemental composition and higher heating value (HHV) were evaluated, and the results are provided in Fig. 4 and Table S7. Fig. 4 reveals two noticeable regions corresponding to the mild hydrotreated liquid products in the presence and absence of catalyst. In the case with catalyst, the liquid products exhibited moderately lower H/C ratios compared to the feedstock. This indicates that hydrogen was consumed primarily to achieve considerably lower oxygen contents, particularly at higher temperature (300 °C), with an O/C ratio of 0.04 compared to 0.27 without catalyst at 300 °C. These observations are in good agreement with expectations, considering the higher deoxygenation activity in the presence of the catalyst as well as at higher temperatures (300 °C). Wildschut et al. [53] as well as Neha et al. [54] reported higher H/C ratio values (1.2–2) for stabilized real pyrolysis oil obtained at 250 °C and 200 °C using sulfided NiMo/Al_2O_3 and reduced NiMo/zirconia catalysts, respectively. However, they observed higher O/C ratios ranging from 0.2 to 0.4 in the obtained oil. Without catalysts lower O/C ratios were also achieved, but also at the expense of much lower H/C ratios (Fig. 4).

For comparison, the elemental compositions, HHV of feedstock (simulated pyrolysis oil), and liquid products are also provided in Table S7, calculated according to the detected compounds by GC–MS analysis. The HHV was calculated by Channiwala and Parikh's correlation [55]. It was found that the HHV values from mild hydrotreatment at 180 °C and 300 °C catalyzed by NiMo/Al_2O_3 catalyst as well as in the absence of catalyst were 30.8, 40.5, 26.7, and 29.1 MJ kg^{-1}, respectively. Among the liquid products investigated, the stabilized pyrolysis oil catalyzed by the NiMo/Al_2O_3 catalyst at 300 °C gave the highest HHV; however, at 180 °C the values were only slightly different in the presence and absence of catalyst. According to the results, NiMo/Al_2O_3 catalyst in mild hydrotreatment at 300 °C was the most promising catalyst as well as condition that produced deoxygenated liquid product with a markedly high energy ratio where HHV was improved by 58.2% compared to the feedstock. This observation is in line with the results observed in earlier studies [54]. Another interesting observation herein, is some leaching of sulfur (almost 3 wt%) from the catalyst in the catalytic experiment at 180 °C (Table S7). However, sulfur leaching was prevented at 300 °C, where the catalyst apparently had better desulfurization activity. Sulfur leaching makes a sulfided NiMo/Al_2O_3 catalyst more appropriate during co-processing when sulfur is present.

3.2.3. Solids formation

The yields of solid products and char-like material (insoluble solid)

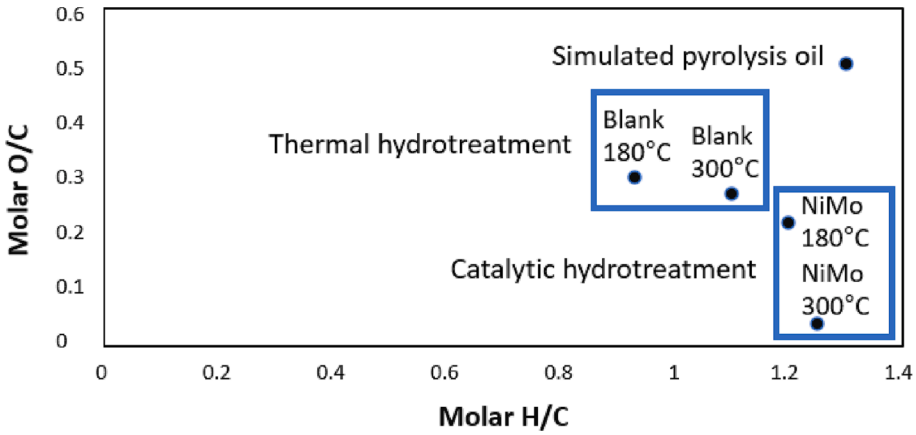

Fig. 4. Van Krevelen plot for the elemental compositions of the liquid products obtained from thermal (blank) and catalytic mild hydrotreatment of simulated pyrolysis oil at 180 °C and 300 °C.

obtained by mild hydrotreatment of the simulated pyrolysis oil are shown in Fig. 5. A comparison of solid yields without and with the catalyst over the reaction temperature range of 180–300 °C reveals a remarkable superiority of the catalyst for reducing the solid yield, particularly at the intermediate temperature of 250 °C with 5.7 wt% solid yield with the catalyst versus 22 wt% in the absence of the catalyst. This solid-suppressing efficiency of the catalyst, corresponding to an almost four-fold reduction in solid yield at higher temperatures, clearly indicates its effect on stabilizing the simulated pyrolysis oil by enabling hydrogenation of reactive free radicals into more stable compounds [56] and thus causing a higher yield of the desired liquid products (Fig. 1d and 2d). However, the higher solid yield mainly at a lower temperature of 180 °C and in the absence of the catalyst (27.4 wt%) provides insight into a lack of means during thermal hydrotreatment to dissociate the hydrogen for hydrogenation reactions to stabilize highly reactive and unstable oxygen-functional groups that are prone to polymerization (Fig. 5a). The solid products were separated into soluble and insoluble fractions using DMSO as an extraction solvent to track the transformation of soluble solids, as an elementary product of polymerization, that could be further polymerized to form insoluble solids. The DMSO soluble solids should be of lower molecular weight compared to the insoluble fraction. Fig. 5b indicates that under catalytic mild hydrotreatment, total solid and insoluble solid yields followed the same descending trend with temperature. Moreover, at all temperatures and in presence of the catalyst, a larger portion of the solid product is DMSO insoluble, particularly at 250 °C where 91% of the solid is made up of insoluble solids. However, at 180 °C the solid consists of close to a 1:1 soluble to insoluble fraction ratio. This reveals that at 250 °C, the catalyst could likely transform the soluble oligomers further into light fractions in the liquid phase and thus suppress its further condensation to a lighter soluble polymer (solid). Therefore, the yield of soluble polymers in the solid product were at a minimum, while at the lower temperature (180 °C) the solubilities of the solid/polymer formed were much higher than those produced at higher temperature. Accordingly, deeper evaluation was performed for the soluble and insoluble fractions to gain a better understanding of their composition. MALDI-TOF and NMR analyses have been applied to determine the average molecular weight (M_w) and structure of the soluble fraction, respectively. Elemental analysis also has been carried out to complement the structural evaluation of the heavier insoluble solid.

3.2.3.1. DMSO soluble solids. The soluble solids were investigated by MALDI-TOF, scanning from 200 to 2000 *m/z*. Their average molecular weight was measured to realize the extent of the polymerization. Furthermore, the average molar mass of one monomer unit from the feedstock mixture is 109 Da, and this is used to estimate the structure of the soluble solid (Table S8). As illustrated in Fig. S7 and Table 2, it is closely associated with the temperature during the mild hydrotreatment as a wide distribution of molecular weights has been found in the soluble solids. The MALDI-TOF analysis presents signals in the ranges 300, 500, 600, 700, 800, 900, and over 1000 *m/z* that corresponded to trimers, pentamers, hexamers, heptamers, octamers, nonamers and macromolecules, respectively (Table S8).

It could be seen in Table 2 that by elevating the temperature, the average M_w of the soluble solid fractions obtained from catalytic hydrotreatment declined from 915 g/mol at 180 °C to 522 g/mol at

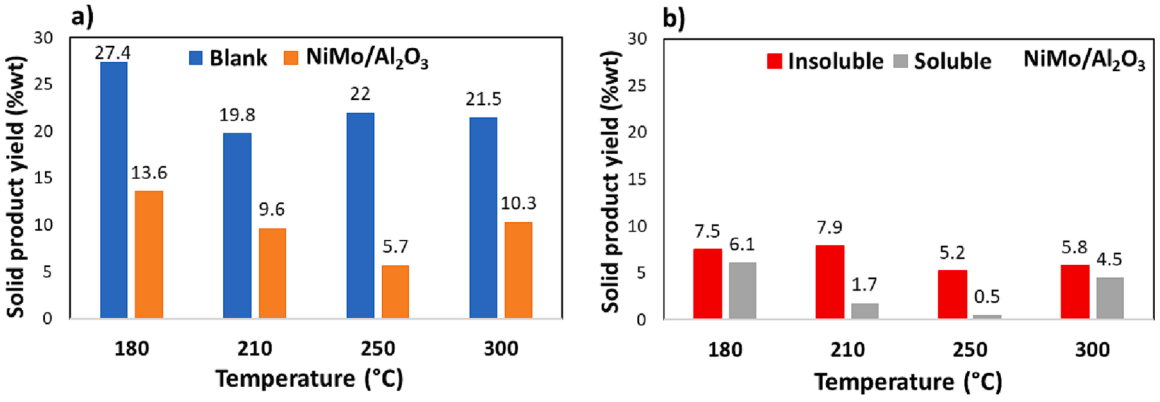

Fig. 5. Effect of temperature on solid product formation in thermal and catalytic hydrotreatment over the $NiMo/Al_2O_3$ catalyst. Reactions were performed under 60 bar H_2 for 4 h. a) total solid product yield during blank and catalytic experiments. b) The yield of soluble and insoluble solid extracts in presence of the catalyst.

Table 2
Properties of soluble and insoluble solids obtained from the conversion of simulated pyrolysis oil at various temperatures (180–300 °C), 60 bar H_2, and reaction time t0 after 13 min ramp to setpoint temperature, t4: temperature ramp and 4 h at constant temperature, in the absence and presence of the NiMo/Al_2O_3 catalyst.

Experiment (Time, h)	Catalyst	Temperature (°C)	Soluble solid	Insoluble solid	
			Average M_w (g/mol)	Molar ratio C/H	Yield (wt%)
t0	NiMo	180	640	0.4	3.2
t4	Blank	180	854	1	23.3
t4	NiMo	180	915	0.7	7.5
t4	NiMo	210	585	0.9	7.9
t4	NiMo	250	564	0.9	5.2
t4	NiMo	300	522	1	5.8
t4	Blank	300	–	1.1	21.5

300 °C. They also have a relatively higher molecular weight compared to that without adding the catalyst, e.g., 854 g/mol at 180 °C, which is probably linked to the effect of the catalyst in producing more solid product rich in soluble polymers rather than char during mild hydrotreatment. Hence apart from temperature, the catalyst also had some effect on the structure and the molecular weight of the soluble fraction. Also, of interest is to characterize differences in the molecular weight distributions of the soluble solid fractions. As shown in Fig. S7, MALDI results obtained by adding the NiMo/Al_2O_3 catalyst implies that at low temperature (180 °C), there is a very broad M_w distribution from 500 and greater than 1000 in which the main compounds in the soluble solid are pentamers (551.3 *m/z*), heptamers (713.6 *m/z*), and nonamers (995.5 *m/z*), as well as macromolecules (over 1000 *m/z*). However, at higher temperatures, the M_w distribution shifts towards lower M_w compounds so that no macromolecules are observed, and most compounds are less than M_w of 500, thus mainly trimers. Instead, in the absence of the catalyst, at 180 °C the soluble solid is rich in groups of hexamers, heptamers, octamers and nanomers but with less intensive signals compared to that with the catalyst.

Various functional groups in the soluble solid fractions obtained at two temperatures, 180 and 300 °C were characterized based on the chemical shift distributions. Two dimensional-^{1}H–^{13}C-HSQC NMR was used to avoid overlapping peaks, occurring for some compounds via spreading of the signals into two dimensions (Fig. 6). Initially, the feedstock (simulated pyrolysis oil) was characterized through 2D-HSQC-NMR analysis (Fig. S8) for comparison to the products. Yu et. al applied the same method to characterize real pyrolysis oil derived from pine wood via dividing the NMR spectra into several chemical shift regions [57]. The HSQC spectrums derived from soluble solids are assigned to different C-H bonds. The aliphatic C-H bonds, sugars, aromatic C-H bonds, and esters give signals at approximately δC/δH 5–55/0.5–3.8, 48–105/3–5.5, 110–125/6.2–7.5, and 122–135/6.7–7.8 ppm respectively. For the aliphatic region, methyl carbons on the aromatic rings typically appear from 10 to 25 ppm, whereas the region from 25 ppm to 38 ppm is related to –CH_2– groups on aromatic side chains attached to a keto-ending group. In addition, for the sugar region, from δC/δH regions of 45 to 80/3–4, 65 to 90/3.5–5, and 95 to 115/4.2–5.5 can be assigned to complex saccharides, oligosaccharides, and disaccharides respectively [58–60]. The possible structures in each group are indicated in Fig. 6. Different functional groups were distinguished by marking the chemical shift regions in the specific area obtained on the basis of our experiments and previous studies [57,61–63]. Comparing Fig. 6a and 6b shows that the soluble solid structure at low temperature (180 °C) is quite different from that of higher temperature (300 °C). At lower temperature (180 °C), the soluble solid products contained sugars, aliphatic and aromatic compounds which were rich in sugar derivatives (Fig. 6a) in accordance with the sugar region in 2D-HSQC-NMR analysis done on fast pyrolysis oil previously [57]. Kadarwati et al. also reported the contribution of sugars in polymerization and thereby formation of solids during stabilization of fast pyrolysis oil using Ru/C [46]. The sugar products comprise disaccharides, oligosaccharides, and complex

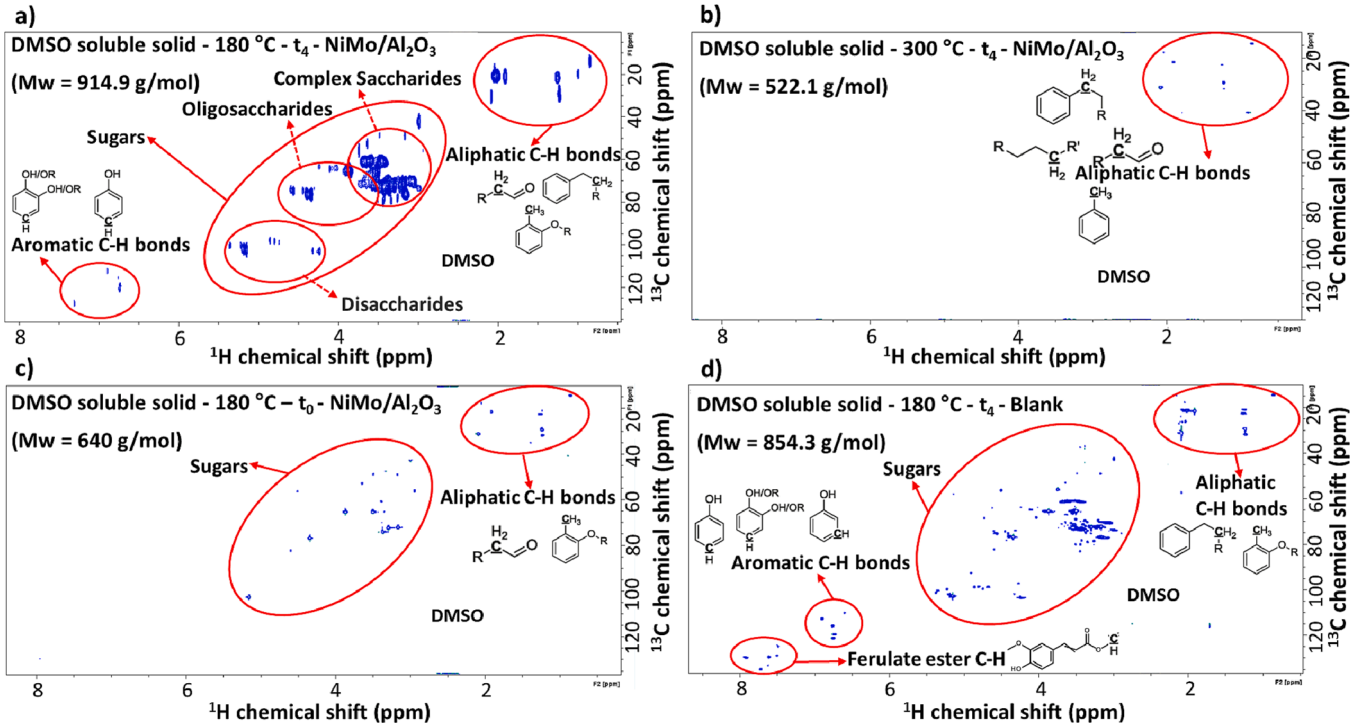

Fig. 6. 2D-HSQC-NMR analysis of soluble solid obtained from mild hydrotreatment in the presence of the catalyst a) 180 °C, t4, b) 300 °C, t4 c) 180 °C, t0, in the absence of the catalyst (blank) d) 180 °C, t4 (6d-DMSO is the solvent), (reaction time t0 after 13 min ramp to setpoint temperature of 180 °C, t4: temperature ramp and 4 h at constant temperature).

saccharides and the intensity of their peaks is remarkably higher than that of the feedstock (simulated pyrolysis oil), illustrated in Fig. S8. It thereby confirms the occurrence of polymerization reactions during mild hydrotreatment leading to the formation of heavy sugar derivatives which are mainly made up of complex saccharides. However, at 300 °C, the soluble solid product is predominantly in the form of aliphatic hydrocarbons (δC/δH 5–38/0.5–2.5). These results are in line with the MALDI experiments that show that the molecular weight of the soluble solids is higher for 180 compared to 300 °C (Table 2). Moreover, the bio-liquid products mainly consist of oxygen-free compounds at 300 °C. However, at 180 °C the liquid product are mainly furans (Fig. 3), likely originating from the HMF conversion (Fig. 2). Thus, the reactive levoglucosan and hydroxyacetone that have high conversion at 180 °C are presumably contributing both to the large quantity of undetected oligomers in the bio-liquid as well as the large amount of oligosaccharides, and complex saccharides in the soluble solids. It is possible that the Lewis acid sites on both alumina and NiMo might contribute to these reactions. At higher reaction temperature (300 °C), the sugar derivatives and aromatic C-H bonds can decompose through hydrocracking and hydrotreatment [64] and consequently, they completely disappeared from the HSQC spectra. Another possibility could be that their formation is prevented at higher temperature. This leads to a considerable reduction in molecular weight (see MALDI in Table 2) and also a considerably lower amount of aliphatic groups are obtained in the soluble solid product. It reveals sugar chain structures were more sensitive than aliphatic structures to increasing reaction temperature.

3.2.3.2. Insoluble solids (char). The carbon/hydrogen (C/H) ratios of insoluble solids from catalytic experiments are reported in Table 2. The C/H ratios are quite similar for the experiments at 180 °C and at 300 °C without catalyst and are around 1–1.1. This is in agreement with Sun et al. [21] that reported a high carbon content of the insoluble polymer obtained from mild thermal treatment of mixed model compounds of furan and phenol in the absence of a heterogenous catalyst. Different compositions of the insoluble solids obtained from experiments with and without catalyst suggest that the catalyst could effectively stabilize reactive compounds, such as furanic compounds which are a potential group for forming heavy compounds, particularly at higher temperatures. The catalyst facilitates stabilization of radical compounds, thus improving formation into light GC detectable liquid and/or soluble solid products (Fig. 7) via hydrocracking, as well as hydrogenation forming less reactive molecules (alcohols, hydrocarbon) which are less prone to char formation. These explanations are consistent with the GC–MS results (Fig. 3). This resulted in lower char yield as well as lower C/H ratio with the catalyst. According to the elemental analysis data, the char composition depends on the reaction temperature in the presence of a catalyst. Along with the temperature increment from 180 °C to 300 °C, the C/H molar ratio of the insoluble solids increased from 0.7 to 1. However, in the catalyst free (blank) experiments the C/H molar ratio was in the range of 1–1.1 at 180 and 300 °C. This suggests that the char consists of highly polymerized (e.g. polyaromatic) species for all blank experiments and increasingly so for catalytic experiments at higher temperature [64–66]. Furthermore, the hydrogen deficiency in the insoluble fractions resembles that expected for the formation of fully developed char.

The study on mild hydrotreatment of simulated pyrolysis oil at 180–300 °C showed that at higher temperature (especially at 300, but also at 250 °C) a deep hydrogenation occurred forming mostly oxygen-free compounds. Since the aim of this study was to examine milder pretreatment for stabilizing the pyrolysis oil, we have further studied the reactions at 180 °C. Accordingly, the effect of different parameters on solids formation including reaction time and oxygenated compounds present in the simulated pyrolysis oil have been assessed at this temperature and will be discussed in the next sections.

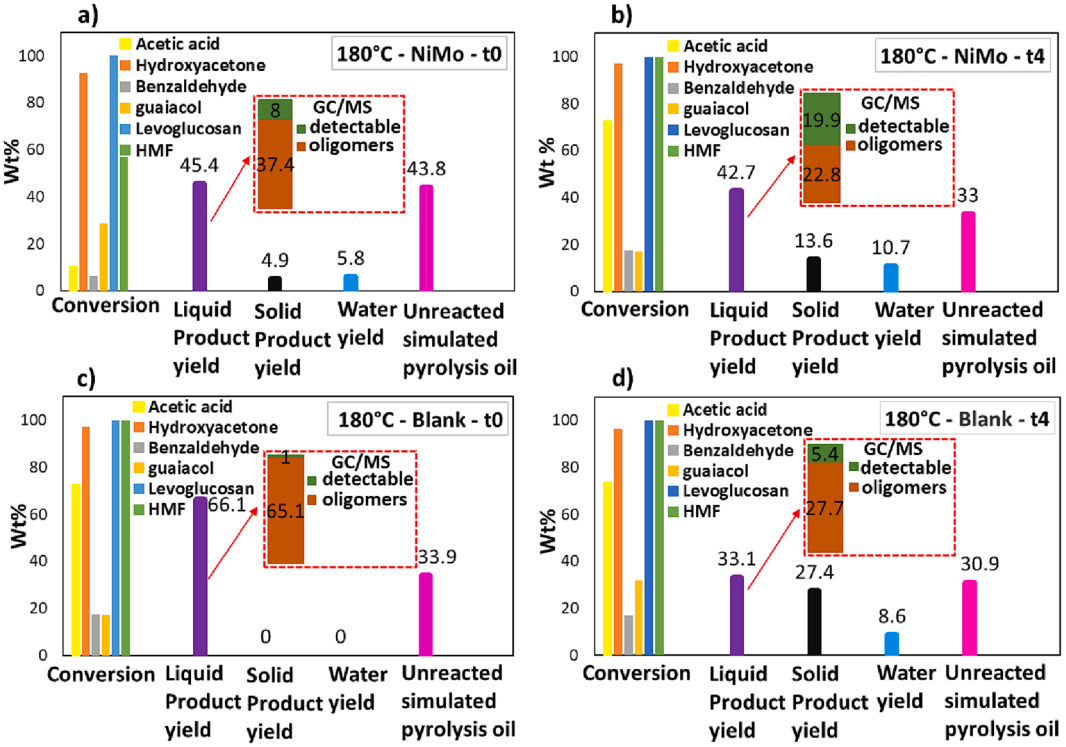

Fig. 7. Effect of heating process on the conversion of oxygenated compounds in simulated pyrolysis oil and product yields (wt%). Reactions performed by first with heating at 12 °C/min from room temperature to 180 °C (t0), followed by 4 h at 180 °C and 60 bar H_2 (t4). a) t0, b) t4 with 1 g $NiMo/Al_2O_3$ catalyst, c) t0 d) t4 without catalyst.

3.3. Effect of heating process on simulated pyrolysis oil conversion and products yield

With the reactor equipment used, increasing the reaction temperature from room temperature to 180 °C, occurred with an average heating rate of 12 °C min^{-1} to reach the set point (approximately 13 min heating period). The pressure increased autonomously during the heating period from 30 bar H_2 to approximately 43 bar at 180 °C. Samples taken after this heating period (and the subsequently cooling process of 10 min) will be labelled as t0. Accordingly, to gain a better understanding of when the solid formation was initiated and its connection to reactant conversion and product selectivity, the mild hydrotreatment of the simulated pyrolysis oil was studied following the heating period (t0) and compared to that following prolongation of the reaction time to 4 h at 180 °C (t4), during which the pressure was set to 60 bar H_2. The temperature profile is illustrated in Fig. S9. Fig. 7a shows that in the presence of the catalyst hydroxyacetone, and levoglucosan had high conversions of 93% and 100% respectively after the temperature rose to 180 °C, whereas benzaldehyde, acetic acid, and HMF conversions still increased with prolonged reaction time from 6, 10, and 57 % after reaching the set point (180 °C) to 18 and 73 and 100 %, respectively after 4 h (Fig. 7b). From t0 to t4 in the presence of the catalyst, the liquid product yield slightly decreased (6%) accompanied by a sharp increase in the water and solid product yields, that more than doubled. Water even started to form during the heating period with a yield of 5.8 wt%, while no water was detected at the same condition in the absence of the catalyst. This can be attributed to the activation of hydrogen in the presence of NiMo metal sites that enhances reactions with oxygenates (hydrogenation-dehydration reactions) and thereby forms water [67]. However, acid sites on the catalyst can also cause condensation reactions contributing to formation of heavy oligomers. The majority of the liquid product obtained up to setpoint (180 °C) using the catalyst was heavy oligomeric products, however following the 4 h reaction the heavy compounds partly decomposed into more light stable fractions, according to the GC–MS results, causing an increase in the yield of the light detectable liquid fraction. It can be reasonably deduced that polymerization was initiated since (i) the acidity of the $NiMo/Al_2O_3$ catalyst could promote the cross-polymerization between reactive components as catalyst acidity is known to strongly influence solid/char formation [30,65]; (ii) the $NiMo/Al_2O_3$ catalyst was not effectively active at a temperature below 180 °C to stabilize highly reactive intermediates by hydrogenation reactions or cleave C-O bonds by hydrogenation and thus hydrocrack heavy oligomers [22]. Therefore, these factors as well as a hot injection of reactants at the setpoint need to be considered to suppress the solid formation at low temperature. The creation of high molecular weight intermediates (GC undetectable fraction) could also have occurred during the approximately 10 min cooling period applied immediately after the heating to be able to withdraw products.

On the other hand, the conversion and product selectivities were strongly different in the absence of the catalyst particularly after the heating period as can be observed in Fig. 7c and d. Compared to the catalytic experiment, among the 6 oxygenated compounds in the simulated pyrolysis oil, only guaiacol was further converted after the 4 h reaction, while others had a comparable conversion. Interestingly, in the absence of the catalyst, no solid formed during the heating process as shown in Fig. 7c (and Fig. S1b), contrary to the catalytic experiment, indicating the promoting effect of the catalyst on solids formation during this stage. It is apparent that without the catalyst at t0, the multiple oxygen group compounds started to form by condensation followed by oligomerization reactions to form soluble oligomers in the liquid phase confirmed by the high yield of heavy oligomeric products (Fig. 7c). However, they did not undergo secondary reactions to be polymerized and separated from the liquid phase in the form of solids. Although they contributed to a high subsequent solid formation only after prolonging the reaction time, reaching 27.4 wt% of solid product yield. In the presence of the catalyst however, the reaction network is more complex with initiation of polymerization of heavy soluble oligomers in the liquid phase due to the acid sites of the catalyst leading to more solid/char formation earlier at t0 (4.9 wt%). Further solid was formed (13.6 wt%) over the 4 h reaction period, but less than for the blank experiment. Another surprising finding was that the acetic acid conversion was significantly lower after heating to 180 °C in the presence of catalyst (10%) compared to without catalyst (73%). Without catalyst, the reactants were transformed into a large amount of oligomers that could not be detected by GC/MS (Fig. 7c). However, no hydrodeoxygenation occurred since no water was formed. For the case with catalyst on the other hand, hydrodeoxygenation started resulting in some water production. Moreover, there was less yield of oligomers in the presence of catalyst, suggesting alternative reaction pathways, suppressing the oligomer formation, possibly by hydrogenation of some reactive species. Moreover, without a catalyst the furans can convert to humins [49–51] as well as undergo ring-opening reactions, producing very reactive species [21,30] and in the case without catalyst this caused a higher conversion of the HMF during heating to t0 (Fig. 7a and 7c). A hypothesis is that in the case without catalyst, the acetic acid reacted with some of the reactive species from HMF decomposition or possibly with the formed oligomers resulting in higher conversion of acetic acid.

The composition of the liquid products according to GC–MS are shown in Fig. 8 for the case without (Fig. 8a) and with (Fig. 8b) the catalyst. According to Fig. 8b, the GC–MS results for light liquid products show that in the presence of the catalyst during the heating process, apart from some partial stabilization reactions via deoxygenation and dehydration, a considerable amount of undesirable condensation reactions also occurred and yielded a large quantity of compounds with multiple oxygen groups due to condensation reactions. The lack of alcohols and low yield of oxygen-free compounds indicate slower hydrogenation activity. The catalyst catalyzes the formation of solid products via liquid heavy oligomers as intermediates. This is evident by the higher yield of solid products directly after heating (Fig. 7a). However, the yield of solid products with the catalyst at t4 is limited by other competing hydrogenation and deoxygenation reactions which become increasingly favored as the temperature approaches 180 °C. The reactions are evident from the higher water yield with the catalyst (Fig. 7a) and yields of light liquid products directly after heating (Fig. 7a and 8b) and extended treatment (Fig. 7b and 8b), as well as the higher yield of oxygen-free products (hydrocarbons) with the catalyst (Fig. 8b), compared to without. On the other hand, without the catalyst, solids form more slowly, but it is far less hindered by competing reactions. The result is first a 74% higher yield of liquid heavy oligomers directly after heating compared to that with the catalyst (Fig. 7c and 7a), which eventually gives a higher yield of solid product but only after the extended treatments at 180 °C (Fig. 7c and b).

As mentioned earlier, without the catalyst, there is higher HMF conversion of more than 60% at t0, compared to the corresponding catalytic experiment (Fig. 7). Therefore, the conversion of furan derivatives (Fig. 8a) can partly contribute to higher yield of heavy oligomers without the catalyst. Whereas with the catalyst HMF conversion is slower and there are higher yields of furans after heating and 4 h at 180 °C and thereby conversions of HMF and furans are more likely to be promoted in the absence of the catalyst. This can be due to reactions with other reactants or reactive intermediates that would either otherwise react with the catalyst or not be present respectively with the catalyst.

Furthermore, higher conversion of guaiacol at t0 with the catalyst and the observation of only low amounts of phenolic compounds by GC–MS suggest the possible effect of phenolic compounds on the polymerization path and thus solid formation. It is followed by partial conversion of multiple oxygen group compounds (with a 45% drop in the yield) and heavy soluble oligomers in the liquid phase into more favorable products (e.g., alcohol, oxygen-free, etc.) via hydrocracking, hydrogenation, hydrodeoxygenation, and dehydration during the

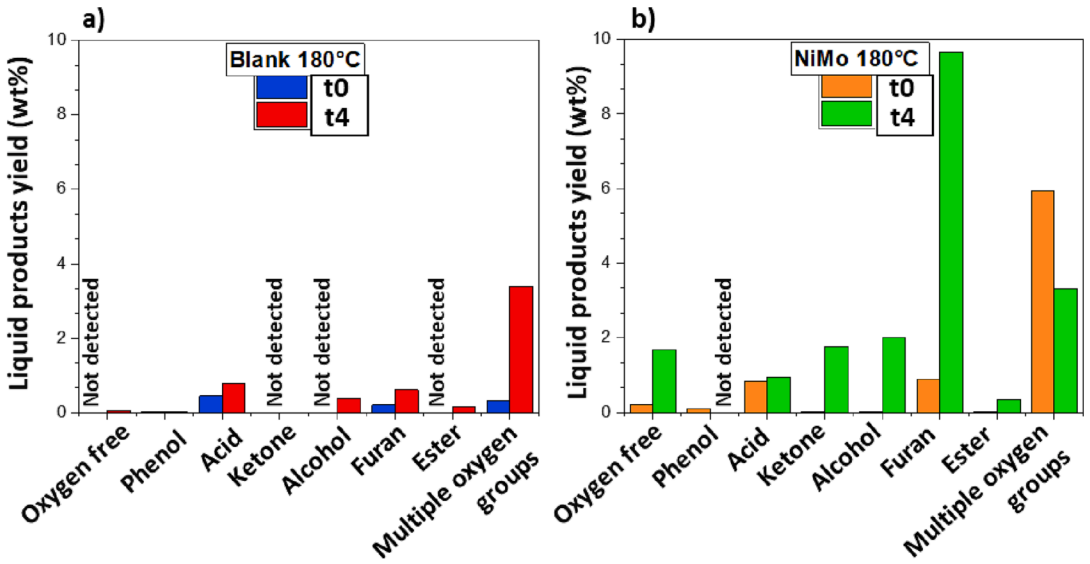

Fig. 8. Light product distribution (wt%) after heating process (t0) and after subsequent 4 h reaction time (t4) for mild hydrotreatment of simulated pyrolysis oil at up to 180 °C, and 60 bar H_2. a) without the catalyst, b) with the NiMo/Al_2O_3 catalyst.

extended 4-hour reaction. It is due to the more effective activity of the catalyst on stabilizing reactive compounds over the 4 h reaction. Therefore, the catalyst suppresses eventually solid formation even during heating period due to the lower yield of heavy oligomers compared to the corresponding blank experiment. Furthermore, it could suppress and reduce solid formation by prolonging the reaction time due to hydrocracking of heavy oligomers compared to the blank experiment under the same reaction condition. However, part of heavy soluble oligomers in the liquid phase are difficult to crack even with the extended (4 h) reaction time and are therefore retained in the liquid product, which also was observed by Kadarwati et al. [46].

On the other hand in the absence of the catalyst by increasing the reaction time, dehydration reactions also occurred that could be due to esterification or other condensation [68]. This result was indicated by the increased yield of multiple oxygen group compounds and sustained high yield of the heavy oligomers in the liquid phase. As a result, among different reactions that are competing simultaneously[5] in the initial heating period, the polymerization path producing solids only occurred during the catalytic hydrotreatment process.

Interestingly, the physical appearance of the two liquid samples obtained after heating to the setpoint (180 °C) with and without the catalyst was completely different as depicted in Fig. S6b. In the absence of the catalyst, the liquid phase consists of a very low yield of furanic compounds and few multiple oxygen group compounds, whereas in the presence of the catalyst higher contents of furans and sugar compounds were detected by GC–MS, which could explain the quite clear and the yellow liquid solution obtained from thermal and catalytic hydrotreatment respectively. Similar physical appearance was also reported for liquid product (containing furans) obtained from hydrogenation of HMF using Ni–Re/TiO_2 in the earlier work [49]. This is also in agreement with our previous findings regarding the color of the liquid products in Section 3.2.2.

Further evaluation of the solid products formed in these experiments was carried out as demonstrated in Tables 2 and 3 and Fig. S7. The solid product formed during heating with the catalyst is rich in char and prolonging the reaction time increases both the soluble solids as well as the char, although the soluble solids increase more. However, the formed insoluble char in the two cases have different properties. As illustrated in Table 2, insoluble solids (char) obtained at t0 in the presence of the catalyst exhibited a C/H ratio of 0.4 (determined by CHOS elemental analysis), suggesting that the char is still not fully developed. Afterward, the C/H ratio approximately doubled by

Table 3
Effect of heating process (t0) and subsequent 4 h reaction at 180 °C (t4) and 60 bar H_2 on total solids and insoluble solids (char) formation.

Time (h)	Blank- Yield (wt%)			NiMo/Al_2O_3 catalyst- Yield (wt%)		
	Total solid product	Char fraction	Soluble solid fraction	Total solid product	Char fraction	Soluble solid fraction
t0	0	0	0	4.9	3.2	1.7
t4	27.4	23.3	4.1	13.6	7.5	6.1

prolonging the reaction time, indicating further polymerization. Thereby a gradual enrichment of the char with carbon was found. In the absence of the catalyst, the char fraction was also the majority (85 %) of the solid product after the 4 hr reaction period. The distribution of M_w in soluble solid at t0 with the catalyst shows that mainly pentamers and hexamers formed with an average M_w of 640 g/mol and then these compounds further grew or combined by prolonging the reaction time to form larger structures like nanomers and even macromolecules as well, with an average M_w of 915 g/mol (Fig. 6 and S7). According to the 2D-HSQC-NMR analysis of the soluble solid products, as can be seen in Fig. 6c, the NMR spectra collected after the heating process in the presence of the catalyst showed two main regions, aliphatic C-H bonds, and sugars, while aromatic C-H bonds are absent. These results illustrate that formation of soluble heavy sugar and aliphatic compounds were initiated during the heating process. Despite reaching a higher intensity of these two groups, by prolonging the reaction time, aromatic compounds also appeared in the soluble solids (Fig. 6a). On the other hand, in the absence of the catalyst after the 4 h reaction period, the soluble solid largely contained tetrameric structures with an average M_w of 854 g/mol (Fig. 6d and S7). Similar groups of compounds are present with and without the catalyst in the NMR spectra (Fig. 6a and d), however especially the complex saccharides had higher intensity in the catalyst experiment. In addition, only in the absence of the catalyst after the 4 h reaction, the ferulate ester group was identified in the chemical range 7.5–8 ppm in the ^{1}H NMR dimension and 120–130 ppm in the ^{13}C NMR dimension.

From this part of our study, the significant influence of the heating process on the conversion of oxygenated compounds in simulated pyrolysis oil and the resulting product distribution was observed. Particularly in the presence of the NiMo/Al_2O_3 catalyst, in which carbon loss in the form of solids was initiated earlier, the reaction network at 180 °C

during the 4 h reaction is complicated. Accordingly, adding more information by studying the influence of each oxygenate in a pyrolysis oil during the stabilization process on the product distribution can be informative. Therefore, a set of experiments with and without the catalyst in which each reactant was removed, one by one, were designed. The focus is on the reactions involving the different oxygenated compounds and their conversion to form solids as will be discussed further in Section 3.4.

3.4. Effects of individual oxygenated groups on product yields

3.4.1. Individual oxygenated groups and liquid product composition

To explore more about the effect of the simulated pyrolysis oil composition and the contribution of each oxygenated group on the product distributions during the stabilization process, catalytic hydrotreatment experiments were performed with the $NiMo/Al_2O_3$ catalyst at 180 °C, 60 bar H_2, and 4 h reaction, where one reactant was removed in each experiment. However, in all experiments, the mass of each reactant was 1.2 g and thus the total mass of feedstock was always constant and equal to that for the experiment containing all 6 reactants. For comparison, blank experiments were also conducted at identical reaction conditions. It is worth mentioning that the effect of removing a component along with increasing the amounts of the remaining reactants should simultaneously affect the product distribution. Fig. 9 presents the product distribution in liquid, solid, and water phases for these experiments with (on the right) and without (on the left) the catalyst. The liquid phase consists of the light GC–MS detectable fractions containing remaining reactants after reaction, different light products, and the heavy oligomer products respectively.

Compared to the mild catalytic hydrotreatment of the simulated pyrolysis oil containing all 6 reactants, in the experiment excluding HMF (Fig. 9a), among the other reactants only hydroxyacetone conversion decreased. This could be due to the stronger adsorption of other oxygenated groups and their intermediates on the catalyst surface in its absence or because there are interactions between hydroxyacetone and HMF or its products that promote conversion of hydroxyacetone. Furthermore, its absence suppressed hydrogenation probably due to a decrease in the stabilization of ketones to corresponding alcohols and consequently lower yields of hydrocarbons and alcohols were obtained. Generally, the absence of HMF reduced the yield of light products, whereas condensation and oligomerization reactions were increased, showing higher selectivity towards multiple oxygen group compounds and heavy oligomers. Meanwhile, it is noteworthy to mention that compared to all catalytic experiments (with/without removing any reactant), the highest yield of these heavy oligomer compounds in the liquid phase was obtained by removing HMF. Last but not least, even after removing this furan reactant from the feedstock, furanic compounds in the liquid product were observed since furan can be typically produced as an intermediate product of the catalytic dehydration of sugars [69]. Considering the same comparison but in the absence of the catalyst, upon removing HMF from the feed mixture, there was no obvious change in conversion of other reactants, while like the catalytic experiment HMF removal lowered HDO and hydrogenation reactions and favored production of heavy oligomers. Interestingly, less solids were formed when removing HMF suggesting that some of the formed oligomers did not further transform to char.

The removal of levoglucosan though showed a completely different trend. In presence of the catalyst, the highest conversion of benzaldehyde and hydroxyacetone was found in comparison with other sets of experiments when the sugar was omitted, suggesting levoglucosan's role in inhibiting aldehyde and ketone conversion (Fig. 9b). Herein hydrogenation, HDO, and hydrocracking were promoted, as higher yields of alcohols, hydrocarbons, and light fractions such as esters were achieved compared to when all 6 reactants were present. The sugar removal was also accompanied by a reduction in the rate of condensation and polymerization reactions that suppressed the formation of higher molecular weight compounds as well as decreased the solid formation significantly. Furthermore, the sugar removal correlated to an improvement in aldehyde and ketone conversion, and thus the selectivity towards corresponding alcohol and hydrocarbon products rose. Additionally, a higher yield of light oxygenated compounds was obtained via the enhanced furan yield, esterification, and reduction in multiple oxygen group compounds formed from condensation reaction. Therefore, in the catalytic experiments, the most dramatic difference, favoring deoxygenated light products, was obtained in the absence of the sugar reactant. In sharp contrast for the blank experiment, removing levoglucosan resulted in more heavy oligomer compounds being produced. However, the solid formation simultaneously decreased, although not to the same extent as the oligomers increased. Interestingly, HMF was not fully converted, likely due to the inhibitory effect of other reactants and/or their intermediates.

Upon the removal of hydroxyacetone from the feedstock in the catalytic experiment (Fig. 9c), only small changes in conversions of other reactants were observed. In the blank experiment, however, large amount of HMF remained. Regarding the light product distribution, the yield of furan in the liquid product was enhanced from 0.6 wt% in the presence of all 6 reactants to 5.7 wt%, when excluding the hydroxyacetone, indicating the contribution of hydroxyacetone or some intermediates from it causing furan ring-opening reactions during thermal hydrotreatment. The elimination of acetic acid from the feedstock in both catalytic and blank experiments did not show any significant changes in the product distribution (Fig. 9d). However, its removal decreased HDO reactions with a hydrocarbon (oxygen-free compounds) yield of 0.3 wt%, and a higher yield of heavy compounds was found. The solid formation was quite similar when removing acetic acid, which is in agreement with Xu et al. [30] that reported that organic acids like acetic acid negligibly affect the cross-polymerization and consequently solid formation. Similarly, the removal of guaiacol showed a lower yield of oxygen-free compounds and a higher yield of heavy compounds, and generally no other changes in the product distribution (Fig. 9f) were observed. However, without the catalyst, light phenolic compounds (1.7 wt%) were found in the absence of guaiacol, showing the inhibitory effect of guaiacol on benzaldehyde conversion into these compounds. Aldehyde removal, here as benzaldehyde, had considerable effects on the product distribution (Fig. 9e). Firstly, in the catalytic experiment, no HDO occurred as indicated by the absence of yield of oxygen-free compounds. Secondly, GC–MS results show the lack of acid production in the light liquid product only in the absence of benzaldehyde. This could be due to benzaldehyde oxidation to form acid [70]. Moreover, in the blank experiment the highest yield of the heavy compound in the liquid phase was obtained when aldehyde was excluded. It is evident that the condensation and oligomerization reactions are inhibited by benzaldehyde.

A comparison of blank experiments, done by removing reactants in succession, shows that the solid yield decreased when removing HMF, levoglucosan and hydroxyacetone, and the largest effect was seen when removing HMF followed by levoglucosan. It should be noted that when removing HMF and levoglucosan, even though the solids were decreased, the oligomers (GC undetectable) significantly increased, suggesting that some of the formed oligomers do not further transform to solids when HMF and levoglucosan are not present. In contrast, the elimination of benzaldehyde and guaiacol led to higher solid formation, which could be due to that the other compounds such as HMF and levoglucosan are increased in the feedstock. Overall, it is reasonable to conclude that since acetic acid, hydroxyacetone, HMF, levoglucosan, benzaldehyde, and guaiacol in the feed mixture contain different functional groups, they can play different roles during condensation and polymerization occurring during thermal hydrotreatment due to their distinct capacity for promoting these reactions. Furthermore, the results show that HMF conversion plays an important role in product distribution, particularly solid content.

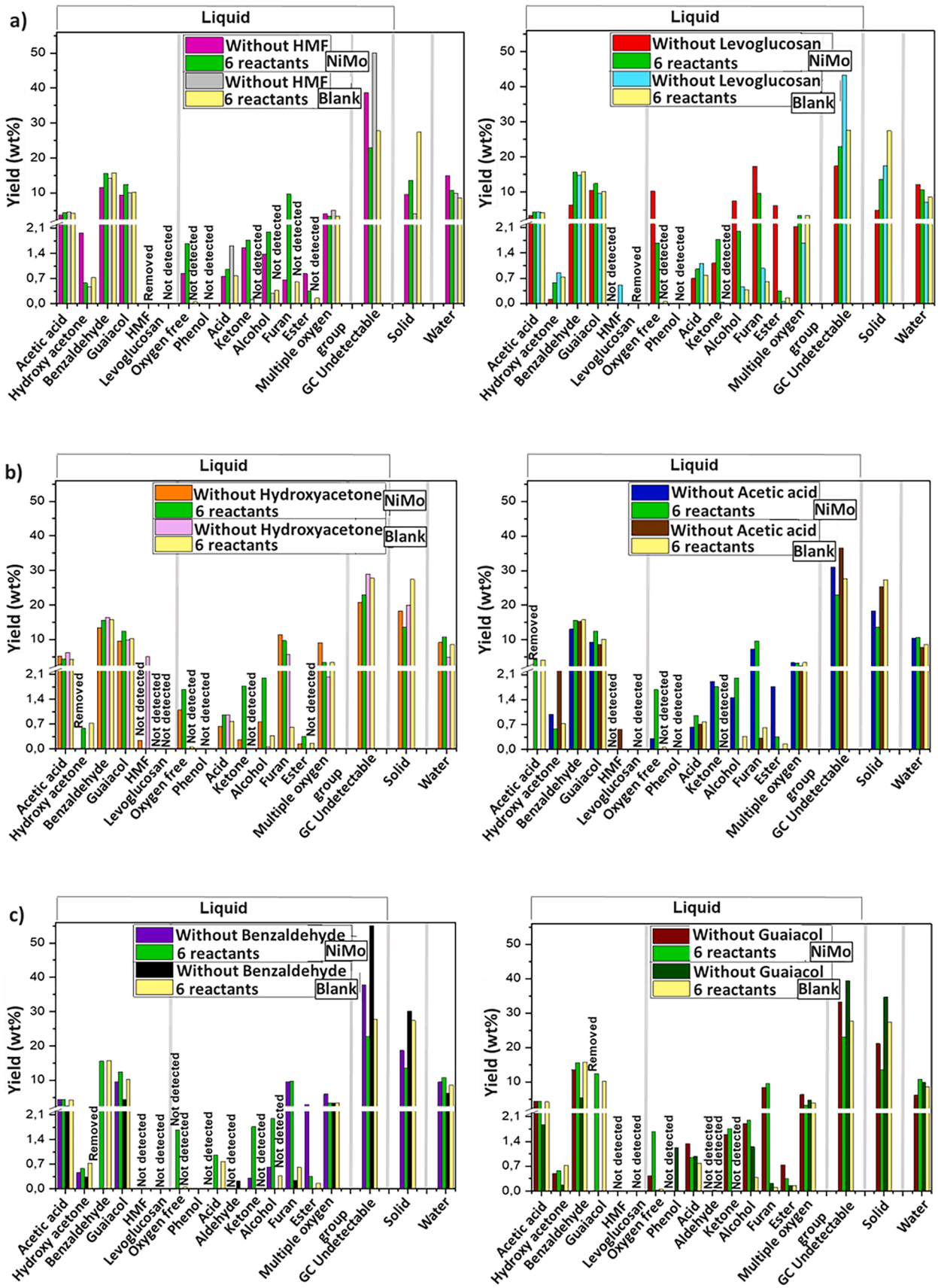

Fig. 9. Effect of removing oxygenated groups on product distribution for mild hydrotreatment of simulated pyrolysis oil at 180 °C, 60 bar H_2, 4 h reaction, with and without the addition of the catalyst. Removal of a) HMF and levoglucosan, b) hydroxyacetone and acetic acid, c) benzaldehyde and guaiacol.

3.4.2. Individual oxygenated groups and solid formation

The influence of different oxygenated groups on the yields of total solid products and insoluble solids during thermal and catalytic mild hydrotreatment of simulated pyrolysis oil is shown in Fig. 10. As mentioned earlier to keep the same quantity of feedstock, upon removal of each compound, the quantity of other compounds was increased. Therefore, the effect of removing a compound and increase of the remaining compounds needs to be considered simultaneously for the interpretation of these experiments. According to the solid yields, the amount of solid/char formed is mainly a function of the reactivity of the oxygenated groups. In blank experiments without the catalyst, the removal of less reactive components and instead excess of more reactive compounds will lead to intensified solid/char formation. Whereas minimum solid is formed when a highly reactive oxygenate e.g., HMF is removed as seen in Fig. 10a. This shows the clear importance of furans (i.e. HMF in our case) in contributing to the solid/char formation in blank experiments at t4. This is because of its known potential for cross-polymerization interactions with other oxygenates like sugars [30]. Therefore, its presence at particularly high levels can be considered a major problem during the stabilization of pyrolysis oil. Its reactivity originates from the aldehyde group attached to the furan ring that activates HMF for aldol condensation reactions and the produced intermediates can continue to polymerize with other reactive oxygenated compounds that eventually form solid/char [32]. It is noteworthy that the opening of the furan ring provides an additional means for which HMF assists polymerization and consequently solids formation. However, as also shown in Fig. 10a, the removal of reactive levoglucosan containing many oxygen groups, caused the greatest reduction in solid formation, for experiments in the presence of the $NiMo/Al_2O_3$ catalyst. This is probably due to the high reactivity of levoglucosan catalyzed by the acidic $NiMo/Al_2O_3$ catalyst, to be hydrolyzed to glucose followed by its further degradation to furans which significantly contributes to the formation of solid/char [50]. This confirms the higher yield of furans detected in the previous catalytic experiment at 180 °C after 4 h reaction (Fig. 3a), where all 6 oxygenated compounds were presented. This suggests that the furans probably also partially formed from levoglucosan, not just HMF and indeed when removing HMF (Fig. 9a) furans were detected in the case of the $NiMo/Al_2O_3$ catalyst.

Interestingly among all catalytic and thermal experiments, the most promising result with the lowest solid yields was obtained in the absence of the catalyst where HMF was removed. The solid obtained from the catalytic experiment excluding HMF showed a distinct composition compared to other catalytic experiments where a large portion (87%) of the solid product was DMSO soluble, whereas in the rest of the

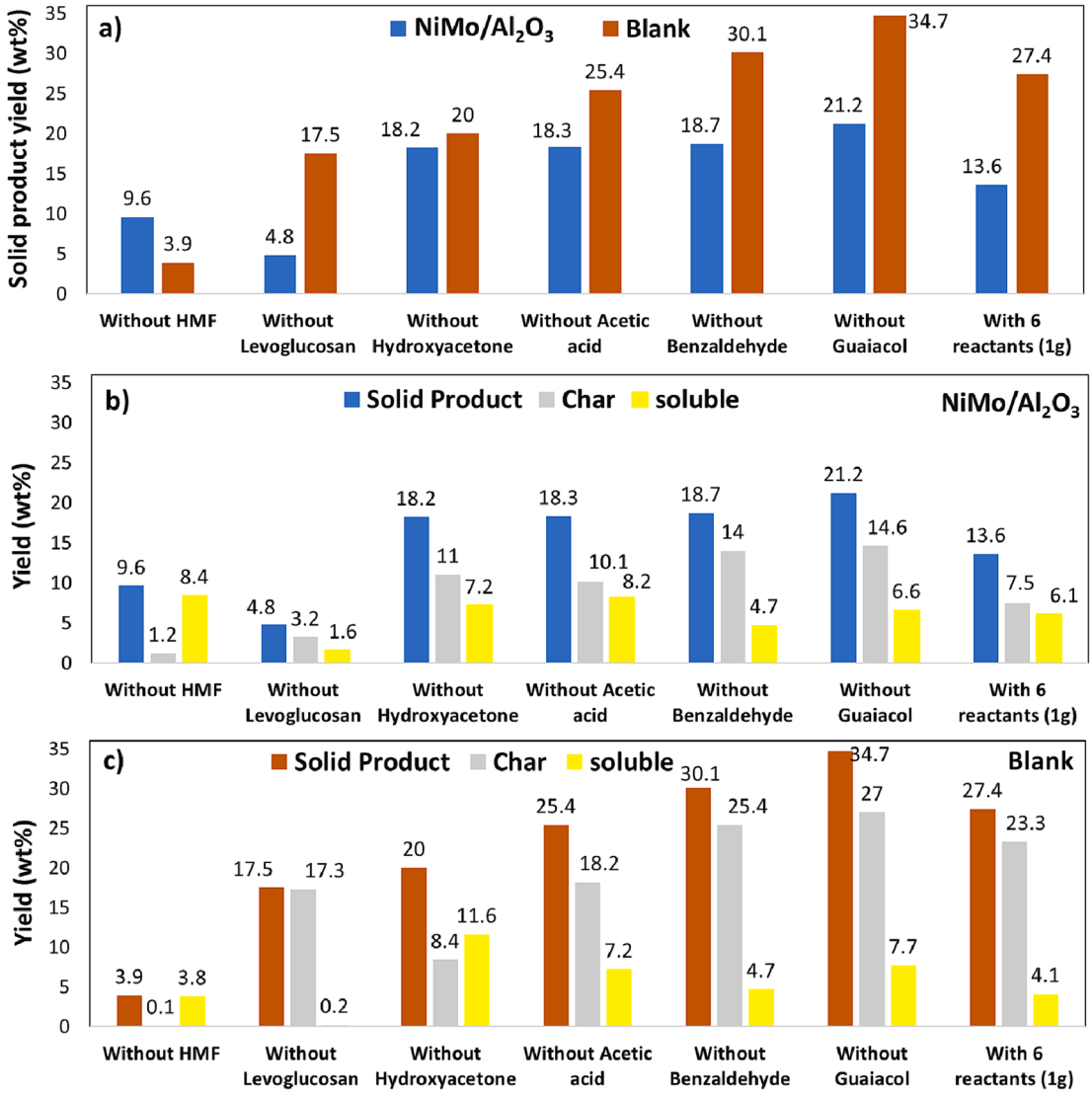

Fig. 10. Effect of components excluded from feedstock on solid product yield in experiments performed at 180 °C, under 60 bar of H2 for 4 h. Solid product yield during blank and catalytic experiments (a). The yield of soluble and insoluble extracts in presence of the catalyst (b), and in the absence of the catalyst (c).

experiments, solids mainly consisted of char (Fig. 10b). It shows that the solubility of the polymers/solids is affected by the type of polymerization reaction, determined by the functionalities of the reacting oxygenated compounds. In the blank experiments, the trend was different for some cases. Removing highly reactive components like HMF and hydroxyacetone from the feedstock mixture resulted in the formation of more soluble solid. On the other hand, excluding levoglucosan, another very reactive component, produced almost only insoluble char residue, with the lowest percentage of the soluble fraction. This indicates that levoglucosan primarily forms the soluble polymer/solid in the absence of the catalyst.

It could be seen in Table 4 and Fig. S7 that the molecular weight distribution patterns were different depending on the removed reactants and the presence of the catalyst. Determination of the structures in the soluble solid fractions from MALDI-TOF showed that the catalytic experiment excluding HMF produced product with the highest average M_w (1187 g/mol), with an extensive distribution of products comprising hexamers, and up to macromolecules. Moreover, the NMR results in Fig. S8 illustrate that sugars and aliphatic compounds were the most prevalent, followed by aromatics and ferulate ester groups. In the same experiment but in the absence of the catalyst, sugars, aromatic and aliphatic compounds with lower peaks intensity and no ester groups were detected which is in line with MALDI-TOF data with a lower average M_w (729 g/mol). This difference in the average M_w of these two soluble solid samples demonstrates that when removing HMF there are larger oligomers present in the soluble solids as well as larger quantities of solids showing that the catalyst enhances the polymerization in this case. However, in the presence of the catalyst, when levoglucosan was removed from the feedstock, the soluble solids decreased significantly, and the structure changed considerably. The soluble solids in this case were mainly composed of pentamers and hexamers with a low intensity of aliphatic and sugar compounds observed from the NMR data (Fig. S8). Herein, the absence of heavier compounds and thereby the lower average M_w, 647 g/mol, could be related to a lower tendency for other oxygenated groups or reactive intermediates to cross polymerize with the sugar [30]. This finding is consistent with the GC–MS data where a lower yield of the heavy oligomers was also obtained in the liquid phase in the absence of the sugar (Fig. 9a). In the blank experiment by the removal of the sugar, soluble solids containing aliphatic compounds with some aromatic compounds could also be faintly detected.

According to MALDI and NMR analyses (Figures S7 and S8) elimination of other oxygenated compounds in both catalytic and blank experiments did not have a pivotal influence on the structure of the soluble solids. To assess the effect of different oxygenated compounds on insoluble solids composition, insoluble fractions obtained from these sets of experiments were analyzed. As illustrated in Table 4, when excluding different oxygenates in the catalytic experiments, the lowest C/H molar ratio of 0.5 and 0.2 was obtained by removing levoglucosan and HMF, respectively, showing that char was not fully developed. However, removing other less reactive oxygenated compounds from the feed mixture in the presence of the $NiMo/Al_2O_3$ catalyst caused an enhanced C/H molar ratio in the region of 0.9, suggesting the formation of more fully developed char. In the absence of the catalyst the C/H ratios were similar and in the range of 0.8 to 1.1, showing that the char was well developed in these cases.

Table 4
Properties of soluble and insoluble solids obtained from the removal of individual compounds for experiments at 180 °C, 60 bar H_2, and reaction time t4: 4 h in the absence and presence of the $NiMo/Al_2O_3$ catalyst.

Component removed	Catalyst	Temperature (°C)	Soluble solid	Insoluble solid	
			Average M_w (g/mol)	Molar ratio C/H	Yield (wt%)
HMF	NiMo	180	1187	0.2	1.2
HMF	Blank	180	729	–	0.1
Levoglucosan	NiMo	180	647	0.5	3.2
Levoglucosan	Blank	180	590	1.1	17.3
Hydroxyacetone	NiMo	180	949	0.8	11
Hydroxyacetone	Blank	180	1059	0.9	8.4
Acetic acid	NiMo	180	801	0.8	10.1
Acetic acid	Blank	180	837	1	18.2
Benzaldehyde	NiMo	180	896	0.8	14
Benzaldehyde	Blank	180	622	1	25.4
Guaiacol	NiMo	180	762	0.9	14.6
Guaiacol	Blank	180	912	0.9	27

3.5. Catalyst reusability test

Industry places importance on the ability to recover and reuse a catalyst, as it significantly contributes to the economic feasibility of scaling up catalytic processes [71]. Accordingly, the recovered catalyst was reused in a recycle run in stabilization of simulated pyrolysis oil (180 °C for 4 h), at identical experimental conditions as used for the fresh catalyst. The product distribution from these two experiments were compared and the results are presented in Fig. 11. It should be noted, as described in the Section 2.2, that repeating of the experiment with fresh $NiMo/Al_2O_3$ resulted in solid yields of 13.6 and 14.1 wt%, respectively, thus the experimental reproducibility is very high. The 75.7 wt% liquid product yield obtained with the fresh catalyst increased to 84 wt% after recycling. However, the water yield was substantially decreased by 50%, suggesting that the reused catalyst underwent a decrease in its HDO capability due to the recycling process. This was also accompanied by a slight reduction in solid yield which was consistent with findings by Oh et al. [72] using a Ru/C catalyst with its first reuse. However, according to their results, the char yield increased with an increase in the recycling number, due to catalyst deactivation, primarily caused by the accumulation of char on the active sites [73].

3.6. Reaction pathway for mild hydrotreatment

The results from different characterization techniques of the formed oil, soluble solids and char are used to propose a reaction pathway during mild hydrotreatment. Scheme 1 illustrates the conversion, cross-linking tendency, and selectivity for various oxygenated compounds through three main possible reaction pathways occurring during mild (180 °C) and more severe (300 °C) hydrotreatment of the simulated pyrolysis oil. The products/intermediates indicated are the most abundantly detected compounds under the tested mild hydrotreatment conditions. The arrows included at 180 °C, indicate which products are most likely formed from which products. The rate of these paths could be varied based on the reaction temperature, time, and presence/absence of the catalyst. During heating up to 180 °C, condensation, and oligomerization reactions primarily between furans, sugars, and aldehydes

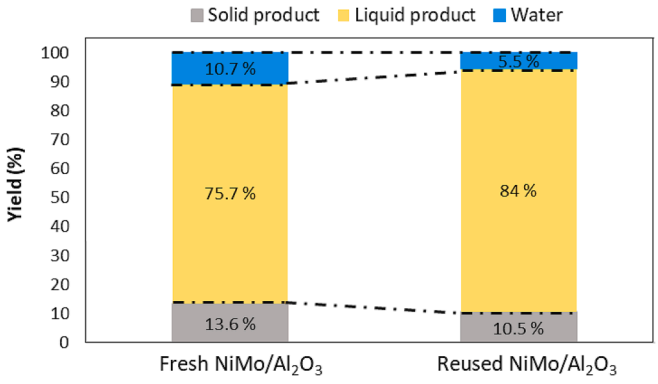

Fig. 11. Product distribution in two runs at 180 °C, 60 bar H_2, for 4 h catalyzed by a) fresh and b) spent $NiMo/Al_2O_3$ catalysts.

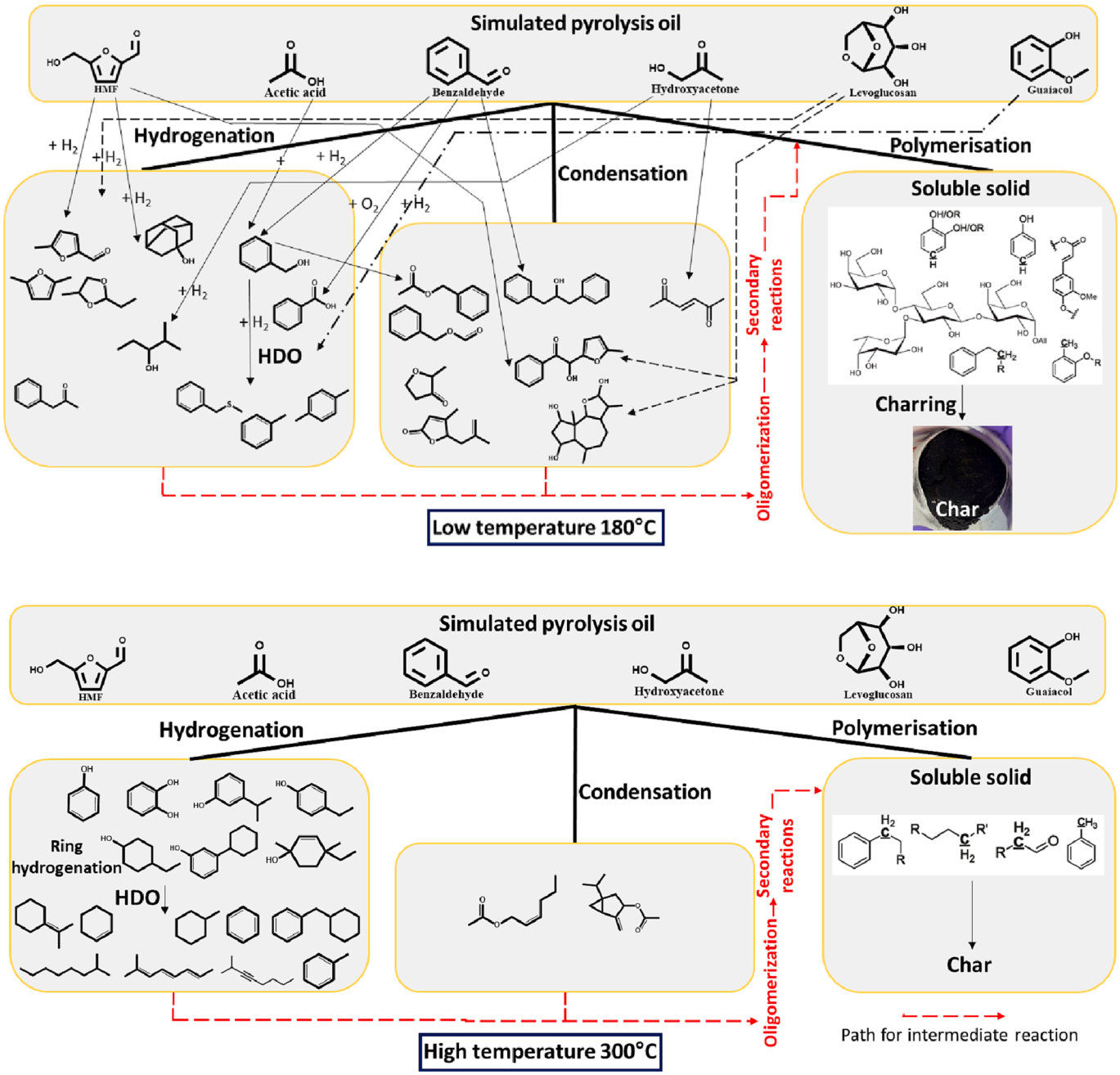

Scheme 1. Proposed main reaction pathways during mild catalytic hydrotreatment of simulated pyrolysis oil.

were dominant, whereas by increasing the reaction time and with catalyst, moderate stabilization occurred via conversion of oxygenated compounds into hydrotreated furans, alcohols, and esters along with polymerization reactions. However, at 300 °C and in the presence of catalyst, the main hydrogenation, condensation and polymerisation pathways are retained however, HDO reactions were more heavily favored. At higher temperature, more monomeric and stabilized products are present in the oil product (mainly hydrocarbons and phenolic compounds). Also, at 300 °C, because the stabilization process has advanced further it is no longer possible to clearly identify what products originate from which reactants.

4. Conclusions

The hydrotreated pyrolysis oil composition resulting from its mild thermal and catalytic hydrotreatment using a conventional sulfided $NiMo/Al_2O_3$ hydrotreatment catalyst was investigated. A comprehensive mixture of various oxygenates, representing the main oxygenated groups in pyrolysis oil, was employed to simulate real pyrolysis oil. The effect of operating conditions including temperatures, heating ramps, and feedstock composition, were assessed in terms of product distributions and composition.

Compared to catalyst-free experiments, our results demonstrated that the increase in the reaction temperature from 180 to 300 °C using the $NiMo/Al_2O_3$ catalyst led to a good stabilization efficiency with improvement in selectivity for stable oxygenates along with notable deoxygenation activity particularly at 300 °C. Contrastingly, in catalyst-free experiments, formation of heavy compounds increased at elevated temperatures mainly due to furan reactions. Although solid product was formed in all experiments, with and without the catalyst, it was about four times lower in the presence of the catalyst, particularly at higher temperatures (250 °C). The NMR, MALDI, and elemental analysis of the

solid products obtained as soluble and insoluble solids by DMSO extraction revealed the chemistry involved in their formation. At 180 °C in the presence of the catalyst, solids were largely made up of highly soluble fractions with macromolecule structures rich in sugar derivatives, that result from polymerization reactions. However, polymerization of sugars was suppressed at 300 °C using the catalyst and soluble solids only consisted of aliphatic compounds with a considerable reduction in their average molecular weight and thereby low yield of soluble solids. It was also found that in contrast to catalyst-free experiments, the insoluble solid composition obtained from catalytic experiments is a function of temperature giving fully developed char only at elevated temperatures. A reaction network was proposed based on the main reaction products in the liquid and solid phases.

Evaluation of the influence of heating up process to 180 °C, with and without catalyst, showed a surprising result. Although the catalyst improved the rate of hydrogenation that should limit the formation of heavy oligomers, it could however catalyze secondary reactions converting oligomers more quickly to soluble solids comprising sugars, aliphatic compounds, and a trace of insoluble solids. However, in the absence of the catalyst a higher degree of condensation reactions occurred due to less hydrogenation, and subsequent polymerization or solid formation occurred more slowly, resulting in that no solids were observed after only heating. However, by prolonging the reaction time without catalyst, the solids increased significantly. But with catalyst a lower solid yield was found after increasing the reaction time at 180 °C, which can be explained by the higher efficiency of the catalyst in suppressing undesired heavy polymer formation.

It was observed that the removal of sugar (i.e. levoglucosan) as well as furan (HMF) from the feedstock in the presence of the catalyst at 180 °C, resulted in a hydrotreated pyrolysis oil with a higher degree of hydrogenation and the lowest solid product formation. Interestingly, the lowest solid formation was obtained under mild hydrotreatment when HMF was omitted with and without catalyst at comparable reaction conditions. These results highlight how furans are most responsible for the extent of solid formation during mild hydrotreatment, due to their potential cross-polymerization tendency with other reactive compounds/intermediates. In addition, they played an important role influencing the nature of solid products, favoring formation of more insoluble solids with higher molecular weight. Furthermore, the inhibitory effect of sugar on the conversion of benzaldehyde and hydroxyacetone was observed. HMF was found to have a promoting effect on hydroxyacetone conversion and vice versa, hydroxyacetone promoted HMF conversion under both thermal and catalytic reaction conditions. The formation of heavy oligomers in liquid products decreased slightly when removing sugars and ketones, suggesting their importance for oligomer formation. Acetic acid and phenols had no effect on the liquid product composition and solid formation at low temperatures (180 °C), which points to their weak effect at these temperatures.

In general, based on our results there can be different strategies to minimize the solid formation. The pyrolysis liquid could be heated fast without a catalyst to avoid solid formation and thereafter inject hot pyrolysis oil into the catalytic bed. However, if the heating is slower then significant solid formation will occur without a catalyst. For this case it would be better to either (i) heat with a catalyst or (ii) remove HMF components before heating without the catalyst, or possibly minimize its formation in the upstream pyrolysis process. If $NiMo/Al_2O_3$ is used as a catalyst, it would be advantageous to convert sugars prior to exposing the bio-liquid to the $NiMo/Al_2O_3$ catalyst. These options could also be combined, starting with removal of furans, thereafter, heating the bio-liquid to convert sugars in a separate pre-treatment reactor with a low temperature active catalyst and thereafter conduct deep hydrodeoxygenation using a $NiMo/Al_2O_3$ catalyst.

CRediT authorship contribution statement

Elham Nejadmoghadam: Conceptualization, Data curation, Formal analysis, Investigation, Writing – original draft. **Abdenour Achour:** Conceptualization, Supervision, Writing – review & editing. **Pouya Sirous-Rezaei:** Supervision. **Muhammad Abdus Salam:** Investigation. **Prakhar Aror:** Conceptualization, Supervision. **Olov Öhrman:** Conceptualization, Supervision, Writing – review & editing. **Derek Creaser:** Conceptualization, Supervision, Writing – review & editing. **Louise Olsson:** Conceptualization, Supervision, Writing – review & editing, Funding acquisition.

Declaration of Competing Interest

The authors declare that they have no known competing financial interests or personal relationships that could have appeared to influence the work reported in this paper.

Data availability

Data will be made available on request.

Acknowledgements

This work has been performed at the Competence Centre for Catalysis (KCK) and the Chemical Reaction Engineering division at the Chalmers University of Technology in collaboration with Preem. The Competence Centre for Catalysis is hosted by Chalmers University of Technology and financially supported by the Swedish Energy Agency (Project No. 52689-1) and the member companies Johnson Matthey, Perstorp, Powercell, Preem, Scania CV, Umicore, and Volvo Group. We would also, like to thank the Swedish NMR Centre for spectrometer time.

Appendix A. Supplementary data

Supplementary data to this article can be found online at https://doi.org/10.1016/j.fuel.2023.129094.

References

[1] Sher F, Curnick O, Azizan MT. Sustainable conversion of renewable energy sources. Sustainability 2021;13:2940. https://doi.org/10.3390/su13052940.
[2] Dada TK, Sheehan M, Murugavelh S, Antunes E. A review on catalytic pyrolysis for high-quality bio-oil production from biomass. Biomass Convers Biorefinery 2023;13(4):2595–614.
[3] Han D, Yin W, Arslan A, Liu T, Zheng Y, Xia S. Stabilization of fast pyrolysis liquids from biomass by mild catalytic hydrotreatment: model compound study. Catalysts 2020;10:402. https://doi.org/10.3390/catal10040402.
[4] Zhang M, Wu Y, Han X, Zeng Y, Xu CC. Upgrading pyrolysis oil by catalytic hydrodeoxygenation reaction in supercritical ethanol with different hydrogen sources. Chem Eng J 2022;446:136952. https://doi.org/10.1016/j.cej.2022.136952.
[5] Yin W, Kloekhorst A, Venderbosch RH, Bykova MV, Khromova SA, Yakovlev VA, et al. Catalytic hydrotreatment of fast pyrolysis liquids in batch and continuous set-ups using a bimetallic Ni–Cu catalyst with a high metal content. Catal Sci Technol 2016;6(15):5899–915.
[6] Hu X, Zhang Z, Gholizadeh M, Zhang S, Lam CH, Xiong Z, et al. Coke formation during thermal treatment of bio-oil. Energy Fuel 2020;34(7):7863–914.
[7] Li Yu, Zhang C, Liu Y, Tang S, Chen G, Zhang R, et al. Coke formation on the surface of Ni/HZSM-5 and Ni-Cu/HZSM-5 catalysts during bio-oil hydrodeoxygenation. Fuel 2017;189:23–31.
[8] Han Y, Gholizadeh M, Tran C-C, Kaliaguine S, Li C-Z, Olarte M, et al. Hydrotreatment of pyrolysis bio-oil: a review. Fuel Process Technol 2019;195:106140.
[9] Dabros TMH, Stummann MZ, Høj M, Jensen PA, Grunwaldt J-D, Gabrielsen J, et al. Transportation fuels from biomass fast pyrolysis, catalytic hydrodeoxygenation, and catalytic fast hydropyrolysis. Prog Energy Combust Sci 2018;68:268–309.
[10] Kim G, Seo J, Choi J-W, Jae J, Ha J-M, Suh DJ, et al. Two-step continuous upgrading of sawdust pyrolysis oil to deoxygenated hydrocarbons using hydrotreating and hydrodeoxygenating catalysts. Catal Today 2018;303:130–5.
[11] Yin W, Wang Z, Yang H, Venderbosch RH, Heeres HJ. Catalytic hydrotreatment of biomass-derived fast pyrolysis liquids using ni and Cu-based PRICAT catalysts. Energy Fuel 2022;36(23):14281–91.
[12] Gong S, Shinozaki A, Shi M, Qian EW. Hydrotreating of jatropha oil over alumina based catalysts. Energy Fuel 2012;26:2394–9. https://doi.org/10.1021/ef300047a.
[13] Grilc M, Likozar B, Levec J. Simultaneous liquefaction and hydrodeoxygenation of lignocellulosic biomass over NiMo/Al2O3, Pd/Al2O3, and Zeolite Y catalysts in

hydrogen donor solvents. ChemCatChem 2016;8:180–91. https://doi.org/10.1002/cctc.201500840.
[14] Yan P, Mensah J, Drewery M, Kennedy E, Maschmeyer T, Stockenhuber M. Role of metal support during ru-catalysed hydrodeoxygenation of biocrude oil. Appl Catal B Environ 2021;281:119470. https://doi.org/10.1016/j.apcatb.2020.119470.
[15] Djandja OS, Wang Z, Duan P, Wang F, Xu Y. Hydrotreatment of pyrolysis oil from waste tire in tetralin for production of high-quality hydrocarbon rich fuel. Fuel 2021;285:119185. https://doi.org/10.1016/j.fuel.2020.119185.
[16] Witsuthammakul A, Sooknoi T. Selective hydrodeoxygenation of bio-oil derived products: ketones to olefins. Catal Sci Technol 2015;5(7):3639–48.
[17] Li K, Wang R, Chen J. Hydrodeoxygenation of anisole over silica-supported Ni2P, MoP, and NiMoP catalysts. Energy Fuel 2011;25(3):854–63.
[18] Bykova MV, Ermakov DY, Kaichev VV, Bulavchenko OA, Saraev AA, Lebedev MY, et al. Ni-based sol–gel catalysts as promising systems for crude bio-oil upgrading: Guaiacol hydrodeoxygenation study. Appl Catal, B 2012;113-114:296–307.
[19] Li X, Gunawan R, Lievens C, Wang Yi, Mourant D, Wang S, et al. Simultaneous catalytic esterification of carboxylic acids and acetalisation of aldehydes in a fast pyrolysis bio-oil from mallee biomass. Fuel 2011;90(7):2530–7.
[20] Gunawan R, Li X, Larcher A, Hu X, Mourant D, Chaiwat W, et al. Hydrolysis and glycosidation of sugars during the esterification of fast pyrolysis bio-oil. Fuel 2012;95:146–51.
[21] Sun K, Zhang L, Xu Q, Zhang Z, Shao Y, Dong D, et al. Evidence for cross-polymerization between the biomass-derived furans and phenolics. Renew Energy 2020;154:517–31.
[22] Gholizadeh M, Gunawan R, Hu X, Kadarwati S, Westerhof R, Chaiwat W, et al. Importance of hydrogen and bio-oil inlet temperature during the hydrotreatment of bio-oil. Fuel Process Technol 2016;150:132–40.
[23] Wan H, Chaudhari RV, Subramaniam B. Aqueous Phase Hydrogenation of Acetic Acid and Its Promotional Effect on *p* -Cresol Hydrodeoxygenation. Energy Fuel 2013;27:487–93. https://doi.org/10.1021/ef301400c.
[24] Boscagli C, Raffelt K, Zevaco TA, Olbrich W, Otto TN, Sauer J, et al. Mild hydrotreatment of the light fraction of fast-pyrolysis oil produced from straw over nickel-based catalysts. Biomass Bioenergy 2015;83:525–38.
[25] Chen J, Wang S, Lu L, Zhang X, Liu Y. Improved catalytic upgrading of simulated bio-oil via mild hydrogenation over bimetallic catalysts. Fuel Process Technol 2018;179:135–42. https://doi.org/10.1016/j.fuproc.2018.06.022.
[26] Xu Y, Li Y, Wang C, Wang C, Ma L, Wang T, et al. In-situ hydrogenation of model compounds and raw bio-oil over Ni/CMK-3 catalyst. Fuel Process Technol 2017;161:226–31.
[27] Guo J, Ruan R, Zhang Y. Hydrotreating of phenolic compounds separated from bio-oil to alcohols. Ind Eng Chem Res 2012;51(19):6599–604.
[28] Kadarwati S, Hu X, Gunawan R, Westerhof R, Gholizadeh M, Hasan MDM, et al. Coke formation during the hydrotreatment of bio-oil using NiMo and CoMo catalysts. Fuel Process Technol 2017;155:261–8.
[29] Xu Q, Sun K, Shao Y, Zhang C, Zhang S, Zhang L, et al. Cross-polymerisation between furfural and the phenolics of varied molecular structure in bio-oil. Bioresour Technol Reports 2019;8:100324.
[30] Xu Q, Zhang L, Sun K, Shao Y, Tian H, Zhang S, et al. Cross-polymerisation between the model furans and carbohydrates in bio-oil with acid or alkaline catalysts. J Energy Inst 2020;93(4):1678–89.
[31] Hu X, Wang Yi, Mourant D, Gunawan R, Lievens C, Chaiwat W, et al. Polymerization on heating up of bio-oil: A model compound study. AIChE J 2013;59(3):888–900.
[32] Hu X, Nango K, Bao L, Li T, Hasan MDM, Li C-Z. High yields of solid carbonaceous materials from biomass. Green Chem 2019;21:1128–40. https://doi.org/10.1039/C8GC03153C.
[33] Wang S, Vorotnikov V, Vlachos DG. A DFT study of furan hydrogenation and ring opening on Pd(111). Green Chem 2014;16:736–47. https://doi.org/10.1039/C3GC41183D.
[34] Pritchard J, Filonenko GA, van Putten R, Hensen EJM, Pidko EA. Heterogeneous and homogeneous catalysis for the hydrogenation of carboxylic acid derivatives: history, advances and future directions. Chem Soc Rev 2015;44:3808–33. https://doi.org/10.1039/C5CS00038F.
[35] Bagnato G, Sanna A, Paone E, Catizzone E. Recent catalytic advances in hydrotreatment processes of pyrolysis bio-oil. Catalysts 2021;11:157. https://doi.org/10.3390/catal11020157.
[36] Shafaghat H, Lee I-G, Jae J, Jung S-C, Park Y-K. Pd/C catalyzed transfer hydrogenation of pyrolysis oil using 2-propanol as hydrogen source. Chem Eng J 2019;377:119986. https://doi.org/10.1016/j.cej.2018.09.147.
[37] Tran C-C, Akmach D, Kaliaguine S. Hydrodeoxygenation of vegetable oils over biochar supported bimetallic carbides for producing renewable diesel under mild conditions. Green Chem 2020;22(19):6424–36.
[38] Farooqui SA, Anand M, Khan A, Kumar R, Khan TS, Haider MA, et al. Noble metal encapsulated sulfide catalyst for the production of aviation biofuel from the hydroprocessing of non-edible oils. Mater Sci Energy Technol 2021;4:413–22.
[39] Payormhorm J, Kangvansaichol K, Reubroycharoen P, Kuchonthara P, Hinchiranan N. Pt/Al2O3-catalytic deoxygenation for upgrading of Leucaena leucocephala-pyrolysis oil. Bioresour Technol 2013;139:128–35.
[40] Abdus Salam M, Wayne Cheah Y, Hoang Ho P, Bernin D, Achour A, Nejadmoghadam E, et al. Elucidating the role of NiMoS-USY during the hydrotreatment of Kraft lignin. Chem Eng J 2022;442:136216.
[41] Dabros TMH, Andersen ML, Lindahl SB, Hansen TW, Høj M, Gabrielsen J, et al. Hydrodeoxygenation (HDO) of aliphatic oxygenates and phenol over NiMo/MgAl2O4: reactivity, inhibition, and catalyst reactivation. Catalysts 2019;9(6):521.
[42] Gunawan R, Li X, Lievens C, Gholizadeh M, Chaiwat W, Hu X, et al. Upgrading of bio-oil into advanced biofuels and chemicals. Part I. Transformation of GC-detectable light species during the hydrotreatment of bio-oil using Pd/C catalyst. Fuel 2013;111:709–17.
[43] Wildschut J, Arentz J, Rasrendra CB, Venderbosch RH, Heeres HJ. Catalytic hydrotreatment of fast pyrolysis oil: model studies on reaction pathways for the carbohydrate fraction. Environ Prog Sustain Energy 2009;28:450–60. https://doi.org/10.1002/ep.10390.
[44] Li S, Zhang S, Feng Z, Yan Y. Coke formation in the catalytic cracking of bio-oil model compounds. Environ Prog Sustain Energy 2015;34:240–7. https://doi.org/10.1002/ep.11936.
[45] Shao S, Zhang H, Xiao R, Shen D. Catalytic conversion of furan to hydrocarbons using HZSM-5: coking behavior and kinetic modeling including coke deposition. Energy Technol 2017;5:111–8. https://doi.org/10.1002/ente.201600100.
[46] Kadarwati S, Oudenhoven S, Schagen M, Hu X, Garcia-Perez M, Kersten S, et al. Polymerization and cracking during the hydrotreatment of bio-oil and heavy fractions obtained by fractional condensation using Ru/C and NiMo/Al2O3 catalyst. J Anal Appl Pyrolysis 2016;118:136–43.
[47] Nolte MW, Saraeian A, Shanks BH. Hydrodeoxygenation of cellulose pyrolysis model compounds using molybdenum oxide and low pressure hydrogen. Green Chem 2017;19:3654–64. https://doi.org/10.1039/C7GC01477E.
[48] Wang H, Rogers K, Zhang H, Li G, Pu J, Zheng H, et al. The effects of catalyst support and temperature on the hydrotreating of waste cooking oil (WCO) over CoMo sulfided catalysts. Catalysts 2019;9(8):689.
[49] Wiesfeld JJ, Kim M, Nakajima K, Hensen EJM. Selective hydrogenation of 5-hydroxymethylfurfural and its acetal with 1,3-propanediol to 2,5-bis(hydroxymethyl)furan using supported rhenium-promoted nickel catalysts in water. Green Chem 2020;22:1229–38. https://doi.org/10.1039/C9GC03856F.
[50] Hu X, Li C-Z. Levulinic esters from the acid-catalysed reactions of sugars and alcohols as part of a bio-refinery. Green Chem 2011;13:1676. https://doi.org/10.1039/c1gc15272f.
[51] Chuntanapum A, Matsumura Y. Char formation mechanism in supercritical water gasification process: a study of model compounds. Ind Eng Chem Res 2010;49:4055–62. https://doi.org/10.1021/ie901346h.
[52] Muangsuwan C, Kriprasertkul W, Ratchahat S, Liu C-G, Posoknistakul P, Laosiripojana N, et al. Upgrading of light bio-oil from solvothermolysis liquefaction of an oil palm empty fruit bunch in glycerol by catalytic hydrodeoxygenation using NiMo/Al 2 O 3 or CoMo/Al 2 O 3 catalysts. ACS Omega 2021;6(4):2999–3016.
[53] Wildschut J, Mahfud FH, Venderbosch RH, Heeres HJ. Hydrotreatment of fast pyrolysis oil using heterogeneous noble-metal catalysts. Ind Eng Chem Res 2009;48(23):10324–34.
[54] Neha S, Remya N, Pedro SFM, Thybaut JW, da Silva WR, Wisniewski Jr A. Catalytic hydrodeoxygenation of bio-oil obtained from microwave co-pyrolysis of food waste and low-density polyethylene. Process Saf Environ Prot 2022;166:23–9.
[55] Channiwala SA, Parikh PP. A unified correlation for estimating HHV of solid, liquid and gaseous fuels. Fuel 2002;81:1051–63.
[56] Yin W, Gu H, Figueirêdo MB, Xia S, Venderbosch RH, Heeres HJ. Stabilization of fast pyrolysis liquids from biomass by catalytic hydrotreatment using Raney nickel "type" catalysts. Fuel Process Technol 2021;219:106846. https://doi.org/10.1016/j.fuproc.2021.106846.
[57] Yu Y, Chua YW, Wu H. Characterization of pyrolytic sugars in bio-oil produced from biomass fast pyrolysis. Energy Fuel 2016;30:4145–9. https://doi.org/10.1021/acs.energyfuels.6b00464.
[58] Ben H, Ragauskas AJ. Heteronuclear single-quantum correlation-nuclear magnetic resonance (HSQC–NMR) fingerprint analysis of pyrolysis oils. Energy Fuel 2011;25:5791–801. https://doi.org/10.1021/ef201376w.
[59] Yin W, Alekseeva (Bykova) MV, Venderbosch RH, Yakovlev VA, Heeres HJ. Catalytic hydrotreatment of the pyrolytic sugar and pyrolytic lignin fractions of fast pyrolysis liquids using nickel based catalysts. Energies 2020;13(1):285.
[60] Zhang X, Ma H, Wu S, Jiang W, Wei W, Lei M. Fractionation of pyrolysis oil derived from lignin through a simple water extraction method. Fuel 2019;242:587–95. https://doi.org/10.1016/j.fuel.2019.01.083.
[61] Speciale I, Notaro A, Garcia-Vello P, Di Lorenzo F, Armiento S, Molinaro A, et al. Liquid-state NMR spectroscopy for complex carbohydrate structural analysis: a hitchhiker's guide. Carbohydr Polym 2022;277:118885.
[62] Bubb WA. NMR spectroscopy in the study of carbohydrates: Characterizing the structural complexity. Concepts Magn Reson 2003;19A:1–19. https://doi.org/10.1002/cmr.a.10080.
[63] Priharto N, Ronsse F, Prins W, Carleer R, Heeres HJ. Experimental studies on a two-step fast pyrolysis-catalytic hydrotreatment process for hydrocarbons from microalgae (Nannochloropsis gaditana and Scenedesmus almeriensis). Fuel Process Technol 2020;206:106466. https://doi.org/10.1016/j.fuproc.2020.106466.
[64] Guisnet M, Magnoux P. Organic chemistry of coke formation. Appl Catal A Gen 2001;212:83–96. https://doi.org/10.1016/S0926-860X(00)00845-0.
[65] Shao S, Zhang H, Xiao R, Li X, Cai Y. Catalytic conversion of biomass-derivates by in situ DRIFTS: Evolution of coke. J Anal Appl Pyrolysis 2017;127:258–68. https://doi.org/10.1016/j.jaap.2017.07.026.
[66] Zhang H, Shao S, Xiao R, Shen D, Zeng J. Characterization of coke deposition in the catalytic fast pyrolysis of biomass derivates. Energy Fuel 2014;28:52–7. https://doi.org/10.1021/ef401458y.
[67] Achour A, Bernin D, Creaser D, Olsson L. Evaluation of kraft and hydrolysis lignin hydroconversion over unsupported NiMoS catalyst. Chem Eng J 2023;453:139829.
[68] Pujro R, García JR, Bertero M, Falco M, Sedran U. Review on reaction pathways in the catalytic upgrading of biomass pyrolysis liquids. Energy Fuel 2021;35:16943–64. https://doi.org/10.1021/acs.energyfuels.1c01931.
[69] Deshan ADK, Atanda L, Moghaddam L, Rackemann DW, Beltramini J, Doherty WOS. Heterogeneous catalytic conversion of sugars into 2,5-

furandicarboxylic acid. Front Chem 2020;8:659. https://doi.org/10.3389/fchem.2020.00659.
[70] Ball DW, Hill JW, Scott RJ. chapter 14. TThe Basics Gen. Org. Biol. Chem. Saylor, 2011.
[71] Kamalzare M. 10 - Recovery and reusability of catalysts in various organic reactions. In: Maleki ABT-HM and NC for the C of OR, editor. Micro Nano Technol., Elsevier; 2022, p. 149–65. 10.1016/B978-0-12-824527-9.00006-X.
[72] Oh S, Hwang H, Choi HS, Choi JW. The effects of noble metal catalysts on the bio-oil quality during the hydrodeoxygenative upgrading process. Fuel 2015;153:535–43. https://doi.org/10.1016/j.fuel.2015.03.030.
[73] Vogt E, Fu D, Weckhuysen BM. Carbon deposit analysis in catalyst deactivation, regeneration, and rejuvenation. Angew Chemie Int Ed 2023::e202300319.